Parallel evolution of vision among hawkmoth species through the diurnal–nocturnal transition

Tokiho Akiyama

Doctor of Philosophy

Department of Evolutionary Studies of Biosystems,
School of Advanced Sciences,
The Graduate University for Advanced Studies, SOKENDAI

2023

Summary

Light environments differ dramatically between day and night. The transition between diurnal and nocturnal ecology has happened repeatedly throughout evolution in many species, e.g., primates and butterflies. Since between day and night both the intensity and wavelength composition of sky light vary in terrestrial habitats, vision is considered to have adapted to ambient light. The light reception begins when light is absorbed by the visual pigment molecules, which consist of an opsin protein and an 11-*cis* retinal attached to it as the chromophore. Evolution of the amino acid sequence of opsin therefore tunes the visual pigment's absorption spectrum. However, because diurnal–nocturnal transition occurred long time ago and/or the diurnal and nocturnal species are distantly related, the molecular and physiological mechanisms underlying the evolution of visual pigments in a set of closely related species through recent diurnal–nocturnal transition have remained a question.

In this thesis, I focus on hawkmoth family (Lepidoptera: Sphingidae), which appeared around 42.8 million years ago containing both nocturnal and diurnal species, to address the question. The enigmatic phenomena have been reported in hawkmoth vision, i.e., color vision in the nocturnal species and scotopic vision type compound eyes in the diurnal species, implying that they have experienced multiple relatively recent diurnal–nocturnal transitions. Thus, I investigated the visual pigments of five nocturnal and five diurnal hawkmoth species.

I performed RNA sequencing (RNA-seq) from the eyes and brain. I reconstructed a phylogenetic tree of hawkmoth species base on the RNA-seq short-read sequences, and showed that the diurnal lineages had independently emerged at least three times from the nocturnal ancestors. I then identified the three visual opsin genes corresponding to the ultraviolet (UV), short-wavelength (SW), and long-wavelength (LW)-absorbing visual pigments in the transcriptomes of each of all the ten species verified by polymerase chain reaction (PCR) method. Opsin gene duplications and losses have occurred frequently in animals during diurnal–nocturnal transition, but hawkmoths kept their opsin gene repertoire. In addition to the opsin gene repertoire, I found no significant differences in the

expression patterns of opsin genes between the nocturnal and diurnal species by RNA-seq analysis: the *LW* gene is predominantly expressed, while the *UV* and *SW* genes are expressed almost equally in hawkmoth eyes.

I constructed the gene trees of opsins, and found that the topology of the UV opsin tree reflects the species' phylogenetic relationships, but in contrast, the SW and LW opsin trees exhibit distinct branching patterns from that of the species tree: SW and LW opsins in diurnal species form monophyletic groups in both trees. The evolutionary rates of amino acid substitutions were significantly higher on the diurnal branches than on the nocturnal branches in all the three opsins. I found an excess number of parallel amino acid substitutions in the opsins in the three independent diurnal lineages, which included the common substitutions on the three diurnal branches. The numbers were significantly more than those inferred from neutral evolution, suggesting that positive selection acted on these parallel substitutions during the transitions.

I measured the spectral sensitivity of the compound eyes by recording the electroretinograms (ERGs), and observed the histological localization of the screening pigments in the eyes in two nocturnal and two diurnal species belonging to different clades. I then predicted the visual pigments' absorption spectra. In the diurnal species, the peak absorption wavelength (λ_{max}) values of SW pigments shifted about 10 nm on average to the long-wavelength direction: 16.0 nm shift for diurnal *C. hylas* and 5.0 nm shift for diurnal *M. pyrrhosticta* from the average value of nocturnal species, respectively. On the other hand, the shift direction was opposite in LW pigments, i.e., the λ_{max} values were about 10 nm shorter in diurnal species: 14.7 nm shift for *C. hylas* and 5.8 nm shift for *M. pyrrhosticta* from the average value of nocturnal species, respectively. Meanwhile, the λ_{max} values of UV pigments were conservative. The reduced λ_{max} separation increases the overlap of the spectral sensitivities of LW and SW pigments, which potentially enhances the color discrimination in the diurnal species.

In conclusion, the transitions from nocturnal to diurnal ecologies in hawkmoths were accompanied by parallel evolution of amino acid sequences of the visual opsins, which presumably brought spectral

sensitivities of LW and SW pigments closer and enhanced the color discrimination properties of diurnal hawkmoths in ambient light. The findings in this thesis of rapid parallel evolution of opsin visual pigments shed new light on adaptive evolution of vision through diurnal–nocturnal transition.

Contents

Chapter 1. General Introduction

Evolution of the light perception has made organisms synchronize circadian rhythms with a 24-hour cycle of the external environment, detect a light direction for phototaxis, recognize objects as vision, etc. (Land and Nilsson, 2012). Vision, in particular, utilizes light information in a variety of ways to govern the behavior, i.e., forming image, detecting motion, color discrimination, sensing brightness, and depth perception. The main sensory organ as an entrance for vision is eyes, which have evolved in diversity and convergence (Land and Nilsson, 2012).

Evolution of the eyes has been the focus of interest in evolutionary biology ever since Charles R. Darwin described "Can we believe that natural selection could produce, ... , organs of such wonderful structure, as the eye, of which we hardly as yet fully understand the inimitable perfection?" in Chapter VI. Difficulties on Theory of *On the Origin of Species* (1859). In the same chapter, then, "the absence or rarity of transitional varieties" is discussed as another difficulty.

Through the comparative anatomy on the retina and photoreceptor cells of vertebrate eyes, a 'nocturnal bottleneck' hypothesis about evolutionary transition of diel (day–night) niches in mammals is presented by Gordon L. Walls (1942). The 'nocturnal bottleneck' hypothesis proposed that the placental mammalian eyes have evolved in an early history of strict nocturnality during Mesozoic era when the dinosaurs dominated the daylight hours. However, to examine the evolutionary mechanism underlying diurnal–nocturnal transition, there is exactly a difficulty of knowing the "transitional varieties", due to the rarity of the closely related species.

For comparisons between closely related species and/or for a specific time scale linking between microevolution (population divergence to speciation) and macroevolution (global biodiversity), the concept 'mesoevolution' was created by Theodosius G. Dobzhansky (1954), but it seems to be a neglected scale so far (Martin and Richards, 2019). To study the pattern and process of 'mesoevolution' the emphasis on parallel evolution is argued in Abouheif (2008), because parallel evolution would be considered a specific process of evolution in which traits sharing a common developmental basis

recurrently appear or disappear among closely related species due to rapid radiations.

Thus, this thesis aims to contribute to understanding parallel evolution of vision among closely related species through diurnal–nocturnal transition, with a focus on the nocturnal and diurnal hawkmoth species (Lepidoptera: Sphingidae). Why/how hawkmoth vision is spotlighted in my project is introduced in Chapter 2. Before moving on there, I provide basic explanations about four related biological matters: (1) hawkmoth, (2) the visual system of insects (compound eye), (3) the visual pigment (opsin), and (4) adaptive evolution of opsins.

Hawkmoth

Hawkmoth family (Lepidoptera: Sphingidae) is one of the macromoth families, and comprises almost 1,700 species (201 genera) classified into three subfamilies: Macroglossinae, Smerinthinae, and Sphinginae (Kitching, 2013–2022. Sphingidae Taxonomic Inventory, http://sphingidae.myspecies.info/, accessed on 8 March 2022) (Kitching and Cadiou, 2000). They are recently diverging insects (Kawahara et al., 2019), and distributed on every continent except for Antarctica (Kitching and Cadiou, 2000). Hawkmoths have a unique ecology in that most adult species are nocturnal while ones in several genera are strictly diurnal (e.g., *Cephonodes*, *Hemaris*, *Neogurelca*, and *Macroglossum*) (Kawahara et al., 2018). The adults lack ocelli, and generally have elongate and triangular forewings for high-speed flight. Also, the proboscises are usually well-developed and very long, but in some species they are degenerate and lost function (Kishida, 2011).

Compound eye

Compound eyes are the main visual organ of insects, as camera type eyes are that of vertebrates. The compound eye is composed of a lot of ommatidia. An ommatidium typically consists of a cornea, a crystalline cone, and eight or nine photoreceptor cells. These cells elongate microvilli toward the center of ommatidium, and together form a rhabdom. Light coming in from the top of the rhabdom is absorbed by the visual pigments contained in the membrane of the microvilli, and then the light energy

is transduced into neural signals (Nilsson, 1989).

Compound eyes can be roughly classified into two types based on optical differences: apposition type and superposition type, although the components of both types are basically the same. On the one hand, the former type rhabdom is thin and long, which is considered as an ancestral type and broadly possessed by diurnal butterflies. On the other hand, the latter type rhabdom is thick and short, and clear zone is well-developed, which is broadly possessed by nocturnal moths (Nilsson, 1989).

Opsin

Opsins are membrane proteins consisting of around 350 amino acid residues in a row, and have a seven transmembrane (TM) structure similar to that of other GTP binding protein-coupled receptors (GPCRs). With an 11-*cis* retinal as the chromophore, an opsin protein constitutes a visual pigment, which typically act as light sensors in animals. Light isomerizes the 11-*cis* retinal to the all-*trans* form, the interaction of the visual pigment with the G protein is triggered, and the phototransduction cascade is driven, resulting in receptor potential in the photoreceptor cell. Opsin gene family is divided into seven subfamilies that diversified before divergence between the deuterostomes (including vertebrates) and the protostomes (including insects), so the types of G proteins coupled to vertebrate visual pigments (transducin, G_t) and insect visual pigments (G_q) differ. Differences in the amino acid sequences of opsins result in differences in the absorption spectra of the visual pigments. Gene duplication is also occurring within each subfamily, leading to diversification of the light wavelengths absorbed by the visual pigments (Yokoyama, 2000; Terakita, 2005).

Adaptive evolution of opsins

Most mutations in proteins are selectively neutral or strongly deleterious, and usually only a relatively small number of amino acid changes can affect the functions (Kimura, 1968; King and Jukes, 1969). To show whether an evolutionary change of opsin gene is adaptive, therefore, it is necessary not only to identify the sequence change by statistical inference, but also to reveal whether

the sequence change actually cause a functional change of opsin and further whether it can increase fitness on a trait. Because *in vitro* reconstitution of G_q-coupled opsins is technically difficult, the elucidation of the amino acid changes of opsins which shift the absorption spectra of visual pigments is biased primarily toward vertebrates. Case examples which have been largely successful in showing adaptative evolution of opsins include the following: the long wavelength-sensitive (LWS) opsin genes of cichlid fishes have adapted to different water depths or clarity, which drives speciation (Terai and Okada, 2011); the duplicated middle to long wavelength-sensitive (M/LWS) type opsin genes of non-human catarrhines have adapted to their specific ecological condition, i.e., detecting targets (mature fruits, young leaves, predators, and social signals) and different combinations of such factors in forest (Kawamura, 2016).

The visual pigments' absorption spectra in several hawkmoth species have been examined by the electrophysiological measurements of the compound eyes' spectral sensitivity in independent previous studies (van der Kooi et al., 2021). Recent advances in sequencing technology have provided chance to facilitate the sequencing and expression comparison of opsin genes in multiple species. In Chapter 3, I describe a step-by-step approach on how to combine methods for different biological hierarchies of the hawkmoth vision. In Chapter 4, I show the results of phylogenetic relationship of nocturnal and diurnal hawkmoths, expression of the opsin genes, molecular evolution of the opsins, and absorption spectra of the visual pigments. In Chapter 5, from the series of results I discuss the mechanism of parallel evolution of vision among hawkmoth species through the diurnal–nocturnal transition. Finally, I provide conclusions, and also expand discussions to connect with evolutionary studies otherwise than the linear discussion up to that point, in Chapter 6.

Chapter 2. Introduction

Adaptive evolution of the visual system to various light environments is a profound factor in the diversification of organisms, which sometimes drives speciation (Walls, 1942; Terai and Okada, 2011). The transition between diurnal and nocturnal ecology has happened repeatedly throughout evolutionary history (Maor et al., 2017; Kawahara et al., 2018). The light environments differ between clear and cloudy skies during the day, and between full moon and starlight at night. However, the most drastic difference is the light environment between day and night (Johnsen et al., 2006). Since both the intensity and wavelength composition of sky light vary between day and night in terrestrial habitats, the differences in ambient light are considered to have affected the spectral sensitivity of retinal photoreceptors (Cronin et al., 2014).

The visual response starts when the visual pigment molecules in the photoreceptor cells absorb light (Land and Nilsson, 2012). The visual pigment consists of an opsin protein, a GTP binding protein-coupled receptor (GPCR), and an 11-*cis* retinal attached to it as the chromophore (Terakita, 2005). The amino acid sequence of opsin and the type of chromophore determine the visual pigment's absorption spectrum (Yokoyama, 2000).

The repertoire of visual opsin genes has often changed with evolutionary transitions of daily activity patterns (Kawamura, 2011; Liu et al., 2018). For example, the 'nocturnal bottleneck' hypothesis during early mammalian evolution (Walls, 1942; Gerkema et al., 2013) suggests that the common ancestor of vertebrates was diurnal and had color vision based on four cone opsins. Then the ancestors of placental mammals lost two of the four cone opsins and became nocturnal for over 100 million years during the Mesozoic Era. After extinction of the dinosaurs, mammals expanded to be diurnal (Maor et al., 2017). One of the remaining opsin genes then duplicated independently in the common ancestor of catarrhine primates (Old World monkeys, apes and humans) and New World howler monkeys (Surridge et al., 2003).

An analogous example is known in the evolution of lepidopteran insects, moths and butterflies.

Roughly 75–85% of lepidopteran species are nocturnal, but their common ancestor appears to have had a diurnal ecology (Kawahara et al., 2018). In the order Lepidoptera, the common ancestor of Heteroneura became nocturnal around 209.7 million years ago (MYA). An ancestral lineage of butterflies (Papilionoidea) shifted back to a diurnal lifestyle around 98.3 MYA (Kawahara et al., 2019). The common ancestor of butterflies presumably had three opsins, which are duplicated or lost in some species (Briscoe, 2008; Feuda et al., 2016; Sondhi et al., 2021).

However, we know little about the effect of recent diurnal–nocturnal transition on opsin gene evolution. How does such a transition with the drastic light environmental change affect vision? Do the opsin genes evolve rapidly? To approach these questions, we need to analyze the effects of diurnal–nocturnal transitions on opsins in a set of closely related species.

Hawkmoths (Lepidoptera: Sphingidae) provide an ideal opportunity to address these questions. The hawkmoth family appeared around 42.8 MYA and the subtribe Choerocampina appeared around 12.2 MYA (Kawahara et al., 2019), thus the subfamily Macroglossinae containing both nocturnal and diurnal species that are phylogenetically close appeared between these two estimated ages (Pittaway and Kitching, 2000–2022. *Sphingidae of the Eastern Palaearctic*, http://tpittaway.tripod.com/china/china.htm, accessed on 8 March 2022) (Kishida, 2011). Extensive phylogenetic analysis has indicated that the ancestral hawkmoth was nocturnal (Kawahara et al., 2018, 2019). In the subfamily Macroglossinae, some species became diurnal within a short evolutionary time period (Kawahara et al., 2009, 2018; Chen et al., 2021).

The hawkmoths' visual system has been studied extensively. The diurnal Hummingbird hawkmoth, *Macroglossum stellatarum*, the nocturnal Elephant hawkmoth, *Deilephila elpenor*, and the nocturnal Tobacco hawkmoth, *Manduca sexta*, all use color vision for floral foraging (Kelber, 1997; Kelber et al., 2002; Goyret et al., 2008). Both in diurnal and nocturnal species, the compound eyes are the refracting superposition type adaptive to scotopic vision (Nilsson, 1989; Warrant et al., 1999). Such enigmatic phenomena in hawkmoth vision, i.e., color vision in the nocturnal species and scotopic vision type compound eyes in the diurnal species, suggest that they have experienced diurnal–

nocturnal transitions rather recently.

Previous studies on *M. stellatarum* and *M. sexta* have revealed that both possess a set of three opsin genes: ultraviolet-sensitive (UV), short wavelength-sensitive (SW), and long wavelength-sensitive (LW) (Chase et al., 1997; Xu et al., 2013; Kanost et al., 2016). Their opsins presumably carry key information on what happened to the evolution of visual perception at the molecular level during diurnal–nocturnal transition events, which occurred recently relative to the events such as in primates and butterflies.

Therefore, I examine the hawkmoth visual opsins to shed light on how their vision has evolved through the ecological transition from nocturnal to diurnal activities among closely related species. I identified the opsin genes, their expression levels, and possible absorption spectra in multiple hawkmoth species. I show that hawkmoth species most likely have adapted their visual function in parallel during the change in their ecology from nocturnal to diurnal life history.

Chapter 3. Materials and Methods

Samples

For molecular biological experiments, I used ten hawkmoth species (Lepidoptera: Sphingidae): five nocturnal and five diurnal. I caught adult individuals of the following species in almost the same geographic location especially for the diurnal species: nocturnal: *Marumba gaschkewitschii* and *Ambulyx ochracea* in subfamily Smerinthinae; *Ampelophaga rubiginosa* and *Theretra japonica* in subfamily Macroglossinae; diurnal: *Cephonodes hylas*, *Hemaris affinis*, *Neogurelca himachala*, *Macroglossum pyrrhosticta* and *Macroglossum bombylans* in subfamily Macroglossinae. Adult individuals were kept at 25°C under a 14/10 hr light/dark cycle for 1–5 days before use. I also collected the larvae of nocturnal *Daphnis nerii* in subfamily Macroglossinae, and then reared them on the fresh leaves of *Catharanthus roseus* and kept the pupae at 28°C under a 14/10 hr light/dark cycle for 16–22 days. I used the adults within two days after emergence. I sampled two or three individuals for all ten species for RNA-sequencing (RNA-seq) analysis (Table 1).

I performed electrophysiological and histological experiments in two nocturnal and two diurnal species: *M. gaschkewitschii* (n = 20: 18 males and 2 females for electrophysiology; n = 1 male for histology), *C. hylas* (n = 18: 16 males and 2 females for electrophysiology; n = 1 male for histology), *M. pyrrhosticta* (n = 18: 9 males and 9 females for electrophysiology; n = 1 male for histology) and *T. japonica* (n = 19: 14 males and 5 females for electrophysiology; n = 1 male for histology). I selected these species because they belong to different clades of the species tree. The numbers of samples were determined to ensure stable results of analyses. Larvae or adults of these species were caught in the same area as those used for molecular experiments. The larvae were reared on the fresh leaves of their host plants at 25°C under a 14/10 hr light/dark cycle for 3–44 days, and the pupae were stored at 10°C for 2–12 months or left at 25°C for 17–24 days and allowed to emerge at 25°C. The adults were kept for 1–40 days at 10°C under a 14/10 hr light/dark cycle and occasionally fed with 15% sucrose solution, except for *M. gaschkewitschii* that does not take food, until use.

The species names and the classification were based on the literature (Kitching, 2013–2022. Sphingidae Taxonomic Inventory, http://sphingidae.myspecies.info/, accessed on 8 March 2022) (Kitching and Cadiou, 2000; Kishida, 2011). Sex was identified by their genital morphology. Their ecology, such as nocturnal and diurnal, was based on Pittaway and Kitching, 2000–2022. *Sphingidae of the Eastern Palaearctic* (http://tpittaway.tripod.com/china/china.htm, accessed on 8 March 2022); Esaki et al. (1971); Kishida (2011); and my field observations (Table 1).

This research was approved by the animal protocols and procedures committee at The Graduate University for Advanced Studies, SOKENDAI.

Table 1. Hawkmoth sample information surveyed by RNA-seq

Sample ID	Species	Subfamily	Sampling location	Sampling date	Sampling method	Collector	Sex	Ecology	Tissues	Fixation date & time	No. of reads	Experiment accession no.	Run accession no.
Mga1	*Marumba gaschkewitschii echephron* (Boisduval, 1875)	Smerinthinae	Yokosuka, Kanagawa, Japan (35°15'N, 139°37'E)	28/07/2014	Adult collection	T.A.	Male	Nocturnal	Adult eyes & brain	31/07/2014 12:00-13:00	27,175,728	DRX229139	DRR239257
Mga2	*Marumba gaschkewitschii echephron* (Boisduval, 1875)	Smerinthinae	Yokosuka, Kanagawa, Japan (35°15'N, 139°37'E)	28/07/2014	Adult collection	T.A.	Male	Nocturnal	Adult eyes & brain	01/08/2014 12:00-13:00	31,977,640	DRX229140	DRR239258
Mga3	*Marumba gaschkewitschii echephron* (Boisduval, 1875)	Smerinthinae	Yokosuka, Kanagawa, Japan (35°15'N, 139°37'E)	28/07/2014	Adult collection	T.A.	Male	Nocturnal	Adult eyes & brain	01/08/2014 12:00-13:00	30,222,302	DRX229141	DRR239259
Aoc1	*Ambulyx ochracea* Butler, 1885	Smerinthinae	Yokosuka, Kanagawa, Japan (35°15'N, 139°37'E)	21/07/2014	Adult collection	T.A.	Male	Nocturnal	Adult eyes & brain	24/07/2014 12:00-13:00	33,952,206	DRX229142	DRR239260
Aoc2	*Ambulyx ochracea* Butler, 1885	Smerinthinae	Yokosuka, Kanagawa, Japan (35°15'N, 139°37'E)	24/07/2014	Adult collection	T.A.	Male	Nocturnal	Adult eyes & brain	29/07/2014 12:00-13:00	28,472,930	DRX229143	DRR239261
Aoc3	*Ambulyx ochracea* Butler, 1885	Smerinthinae	Yokosuka, Kanagawa, Japan (35°15'N, 139°37'E)	28/07/2014	Adult collection	T.A.	Male	Nocturnal	Adult eyes & brain	31/07/2014 12:00-13:00	28,297,454	DRX229144	DRR239262
Chy1	*Cephonodes hylas hylas* (Linnaeus, 1771)	Macroglossinae	Higashikurume, Tokyo, Japan (35°45'N, 139°32'E)	31/08/2014	Adult collection	T.A.	Male	Diurnal	Adult eyes & brain	01/09/2014 12:00-13:00	19,708,896	DRX229145	DRR239263
Chy2	*Cephonodes hylas hylas* (Linnaeus, 1771)	Macroglossinae	Higashikurume, Tokyo, Japan (35°45'N, 139°32'E)	13/09/2015	Adult collection	T.A.	Male	Diurnal	Adult eyes & brain	14/09/2015 12:00-13:00	27,273,782	DRX229146	DRR239264
Chy3	*Cephonodes hylas hylas* (Linnaeus, 1771)	Macroglossinae	Higashikurume, Tokyo, Japan (35°45'N, 139°32'E)	14/09/2015	Adult collection	T.A.	Male	Diurnal	Adult eyes & brain	15/09/2014 12:00-13:00	28,864,550	DRX229147	DRR239265
Haf1	*Hemaris affinis* (Bremer, 1861)	Macroglossinae	Hayama, Kanagawa, Japan (35°15'N, 139°36'E)	06/08/2014	Adult collection	T.A.	Male	Diurnal	Adult eyes & brain	07/08/2014 12:00-13:00	31,536,052	DRX229148	DRR239266
Haf2	*Hemaris affinis* (Bremer, 1861)	Macroglossinae	Hayama, Kanagawa, Japan (35°15'N, 139°36'E)	02/09/2014	Adult collection	T.A.	Male	Diurnal	Adult eyes & brain	03/09/2014 12:00-13:00	29,844,236	DRX229149	DRR239267
Haf3	*Hemaris affinis* (Bremer, 1861)	Macroglossinae	Hayama, Kanagawa, Japan (35°15'N, 139°36'E)	06/09/2015	Adult collection	T.A.	Male	Diurnal	Adult eyes & brain	07/09/2015 12:00-13:00	31,834,506	DRX229150	DRR239268
Nhi1	*Neogurelca himachala sangaica* (Butler, 1876)	Macroglossinae	Yokosuka, Kanagawa, Japan (35°15'N, 139°37'E)	05/08/2014	Adult collection	T.A.	Male	Diurnal	Adult eyes & brain	06/08/2014 12:00-13:00	30,722,512	DRX229151	DRR239269
Nhi2	*Neogurelca himachala sangaica* (Butler, 1876)	Macroglossinae	Higashikurume, Tokyo, Japan (35°45'N, 139°32'E)	31/08/2015	Adult collection	T.A.	Female	Diurnal	Adult eyes & brain	01/09/2015 12:00-13:00	26,655,558	DRX229152	DRR239270
Nhi3	*Neogurelca himachala sangaica* (Butler, 1876)	Macroglossinae	Higashikurume, Tokyo, Japan (35°45'N, 139°32'E)	14/09/2015	Adult collection	T.A.	Female	Diurnal	Adult eyes & brain	15/09/2015 12:00-13:00	29,837,426	DRX229153	DRR239271
Dne1	*Daphnis nerii* (Linnaeus, 1758)	Macroglossinae	Ishigaki, Okinawa, Japan (24°20'N, 124°10'E)	27/09/2014	Larvae rearing	T.A.	Female	Nocturnal	Adult eyes & brain	14/10/2014 12:00-13:00	24,244,384	DRX229154	DRR239272
Dne2	*Daphnis nerii* (Linnaeus, 1758)	Macroglossinae	Ishigaki, Okinawa, Japan (24°20'N, 124°10'E)	27/09/2014	Larvae rearing	T.A.	Female	Nocturnal	Adult eyes & brain	19/10/2014 12:00-13:00	23,958,174	DRX229155	DRR239273
Dne3	*Daphnis nerii* (Linnaeus, 1758)	Macroglossinae	Ishigaki, Okinawa, Japan (24°20'N, 124°10'E)	27/09/2014	Larvae rearing	T.A.	Female	Nocturnal	Adult eyes & brain	20/10/2014 12:00-13:00	25,434,320	DRX229156	DRR239274
Mpy1	*Macroglossum pyrrhosticta* Butler, 1875	Macroglossinae	Hayama, Kanagawa, Japan (35°15'N, 139°36'E)	31/08/2015	Adult collection	T.A.	Male	Diurnal	Adult eyes & brain	01/09/2015 12:00-13:00	30,885,830	DRX229157	DRR239275
Mpy2	*Macroglossum pyrrhosticta* Butler, 1875	Macroglossinae	Hayama, Kanagawa, Japan (35°15'N, 139°36'E)	01/09/2015	Adult collection	T.A.	Male	Diurnal	Adult eyes & brain	02/09/2015 12:00-13:00	36,915,156	DRX229158	DRR239276
Mbo1	*Macroglossum bombylans* Boisduval, 1875	Macroglossinae	Yokosuka, Kanagawa, Japan (35°15'N, 139°37'E)	04/08/2014	Adult collection	T.A.	Female	Diurnal	Adult eyes & brain	05/08/2014 12:00-13:00	22,893,430	DRX229159	DRR239277
Mbo2	*Macroglossum bombylans* Boisduval, 1875	Macroglossinae	Hayama, Kanagawa, Japan (35°15'N, 139°36'E)	11/09/2015	Adult collection	T.A.	Male	Diurnal	Adult eyes & brain	12/09/2015 12:00-13:00	25,896,542	DRX229160	DRR239278
Mbo3	*Macroglossum bombylans* Boisduval, 1875	Macroglossinae	Hayama, Kanagawa, Japan (35°15'N, 139°36'E)	15/09/2015	Adult collection	T.A.	Male	Diurnal	Adult eyes & brain	16/09/2015 12:00-13:00	27,479,356	DRX229161	DRR239279
Aru1	*Ampelophaga rubiginosa rubiginosa* Bremer & Grey, 1853	Macroglossinae	Yokosuka, Kanagawa, Japan (35°15'N, 139°37'E)	21/07/2014	Adult collection	T.A.	Male	Nocturnal	Adult eyes & brain	23/07/2014 12:00-13:00	32,037,438	DRX229162	DRR239280
Aru2	*Ampelophaga rubiginosa rubiginosa* Bremer & Grey, 1853	Macroglossinae	Yokosuka, Kanagawa, Japan (35°15'N, 139°37'E)	21/07/2014	Adult collection	T.A.	Male	Nocturnal	Adult eyes & brain	23/07/2014 12:00-13:00	22,331,642	DRX229163	DRR239281
Aru3	*Ampelophaga rubiginosa rubiginosa* Bremer & Grey, 1853	Macroglossinae	Yokosuka, Kanagawa, Japan (35°15'N, 139°37'E)	28/07/2014	Adult collection	T.A.	Male	Nocturnal	Adult eyes & brain	02/08/2014 12:00-13:00	24,930,292	DRX229164	DRR239282
Tja1	*Theretra japonica* (Boisduval, 1869)	Macroglossinae	Yokosuka, Kanagawa, Japan (35°14'N, 139°35'E)	22/07/2014	Adult collection	T.A.	Male	Nocturnal	Adult eyes & brain	25/07/2014 12:00-13:00	27,381,900	DRX229165	DRR239283
Tja2	*Theretra japonica* (Boisduval, 1869)	Macroglossinae	Yokosuka, Kanagawa, Japan (35°14'N, 139°35'E)	22/07/2014	Adult collection	T.A.	Female	Nocturnal	Adult eyes & brain	25/07/2014 12:00-13:00	33,482,238	DRX229166	DRR239284
Tja3	*Theretra japonica* (Boisduval, 1869)	Macroglossinae	Yokosuka, Kanagawa, Japan (35°14'N, 139°35'E)	25/07/2014	Adult collection	T.A.	Male	Nocturnal	Adult eyes & brain	29/07/2014 12:00-13:00	30,437,216	DRX229167	DRR239285

RNA extraction and sequencing

The eyes and brain tissues were dissected under a dissection microscope and preserved in RNA*later* solution (Ambion, Austin, TX, USA). The dissection was done between 12:00 and 13:00. Total RNAs were extracted from the tissues using the TRIzol reagent (Invitrogen, Carlsbad, CA, USA) following the manufacturer's instructions. From 2 μg of the total RNAs, I purified mRNA by using the NEBNext Poly(A) mRNA Magnetic Isolation Module (New England BioLabs, Ipswich, MA, USA), and constructed the RNA-seq libraries with approximately 400 bp length on average using the NEBNext Ultra RNA Library Prep Kit for Illumina (New England BioLabs) following the manufacturer's instructions. Paired-end reads of 100 bp were determined using an Illumina Hiseq2500 platform (Illumina Inc, San Diego, CA, USA). Short cDNA sequences (2.0–4.0 Gb for each library) were deposited into the DDBJ Sequence Read Archive (DRA) database (accession number: DRA010599) (Table 1).

Reconstruction of hawkmoth species tree

The RNA-seq data from the adult heads of *M. sexta* (accession no.: SRX702703) and *Helicoverpa armigera* (SRX3595764) were downloaded from the European Nucleotide Archive (ENA) database. *H. armigera* was used as an outgroup. The RNA-seq short reads from 12 species (10 from the present study and 2 from the database) were assembled, aligned and concatenated using the SISRS v1.6 software (Schwartz et al., 2015). A phylogenetic tree was inferred by using the Maximum Likelihood (ML) method based on the General Time Reversible (GTR) model of sequence evolution with discrete gamma-distributed rates among sites (Nei and Kumar, 2000), which was selected as the best fit of the nucleotide substitution model in the MEGA v7.0 software (Kumar et al., 2016). All positions with gaps and ambiguous data were removed from the alignment, resulting in 17,305 positions in the final dataset. The reliability of the tree topology was evaluated using 1,000 bootstrap replicates (Felsenstein, 1985). The phylogenetic tree was visualized by the FigTree v1.4.3 program (http://tree.bio.ed.ac.uk/software/figtree/).

Identification of opsin cDNA sequences

After removal of adaptor sequences and low-quality reads (quality score < 0.05), I conducted de novo assemblies of the short cDNA sequences using the CLC genomics workbench 11.0.1 (https://www.qiagenbioinformatics.com/) for each individual. The qualities of the transcriptome assemblies were evaluated by using the Benchmarking Universal Single-Copy Orthologue (BUSCO) v5.4.3 tool with the arthropoda OrthoDB v10 (arthropoda_odb10) dataset of 1,013 single-copy orthologs (Manni et al., 2021). I isolated the homologous partial sequences from the assembled contigs by the BLASTN search (Altschul et al., 1990) using three visual opsin gene sequences from *M. sexta, Manop1* (LW; GenBank accession no.: L78080.1), *Manop2* (UV; L78081.1), and *Manop3* (SW; AD001674.1), as queries. Using the 50 bases of 5′ and 3′-ends of the homologous partial sequences as the queries, I isolated homologous sequences from the RNA-seq reads by the BLASTN search (Altschul et al., 1990) and connected the sequences to both ends of the homologous partial sequences. I repeated this process and then predicted the entire coding region with 5′ and 3′-untranslated regions (UTR) of each species' opsin cDNAs.

I verified the assembled opsin sequences by polymerase chain reaction (PCR). The total RNAs used for RNA sequencing were purified through chloroform extraction and isopropanol precipitation. First-strand cDNAs were synthesized from 1 μg of total RNA using the PrimeScript II 1st Strand Synthesis Kit (TaKaRa Bio Inc., Shiga, Japan). I designed PCR primers on the predicted 5′ and 3′-UTR sequences to amplify the opsin cDNA sequences (Table 2). The cDNAs were used as templates for PCR in a 30 μl solution containing dNTP at 0.25 mM, 0.33 μM of each primer, 0.5 U of Ex Taq HS polymerase (TaKaRa Bio Inc.), and the reaction buffer attached to the polymerase. Reactions for all the primer sets were carried out in a Mastercycler (Eppendorf, Hamburg, Germany) using the same PCR conditions: an initial denaturing step at 93°C for 3 min, 30 cycles of denaturation at 93°C for 1 min, annealing at 55°C for 1 min, extension at 72°C for 2 min, and a final extension step at 72°C for 1 min. The PCR products were purified, and the sequences were determined with the primers for PCR

or sequencing (Table 2) using the BigDye Terminator v3.1 Cycle Sequencing Kit (Applied Biosystems, Foster City, CA, USA) and an Applied Biosystems Automated 3130xl DNA Sequencer (Applied Biosystems, Waltham, MA, USA). The sequences were verified by reading both strands. The opsin cDNA sequences determined in this study were deposited into the international nucleotide sequence database DDBJ/EMBL/GenBank (accession numbers: LC573512–LC573541).

Table 2. List of primers for PCR and sequencing

Gene	Species	Purpose of use		Primer name	Length	Sequences (5' -> 3')
UV	*M. gaschkewitschii*	PCR	External forward	*HUV*_F01	24	AATGGGCCCAGGAGCACTTCACTG
		PCR	External reverse	*HUV*_R01	24	TTAGCAGGTGCAGCCATAGTTGTC
	A. ochracea	PCR	External forward	*HUV*_F02	24	TCCCACAGACAGAAAAAGCTTCCC
		PCR	External reverse	*HUV*_R02	24	CCATTAGAATAGCCATAGTTGTCG
	C. hylas	PCR	External forward	*HUV*_F03	22	GACTGCTCACGTATCCTACAAC
		PCR	External reverse	*HUV*_R03	25	CCATTAAAAAGCCATGGTTGTCGTC
	H. affinis	PCR	External forward	*HUV*_F04	22	GACTGCTCACGTATCCTTCAAC
		PCR	External reverse	Same with *HUV*_R03		
	N. himachala	PCR	External forward	*HUV*_F05	21	ACTCTACTGAGGACTGCTCAC
		PCR	External reverse	*HUV*_R04	24	GTTTAGAGCGTCGAAGTTGAGTTG
	D. nerii	PCR	External forward	*HUV*_F06	22	CACGTAACTTGCAGAACTATCC
		PCR	External reverse	*HUV*_R05	21	CCATCATTAAAGCCGTAGTCG
	M. pyrrhosticta	PCR	External forward	Same with *HUV*_F05		
		PCR	External reverse	*HUV*_R06	22	CATCAGTAAAGCGTTGGTTGTC
	M. bombylans	PCR	External forward	Same with *HUV*_F06		
		PCR	External reverse	*HUV*_R07	24	GTATCGGTTGTCCATCAGTATAGC
	A. rubiginosa	PCR	External forward	*HUV*_F07	25	CTCACGTAACCTGCAAAACTATCCG
		PCR	External reverse	*HUV*_R08	24	CATCAAAAGTCCATCAGTAAAGCC
	T. japonica	PCR	External forward	Same with *HUV*_F05		
		PCR	External reverse	Same with *HUV*_R08		
	All	Sequencing	Internal forward	*HUV*_seqF01	19	ATATGTTCCTGAGGGCTAC
		Sequencing	Internal forward	*HUV*_seqF02	20	GAAATAAGAATAGCCAAAGC
		Sequencing	Internall reverse	*HUV*_seqR01	18	CGCTTCATGGGCAAACAC
		Sequencing	Internall reverse	*HUV*_seqR02	21	AAGCGATGCAAGCGTTAGTCA
SW	*M. gaschkewitschii*	PCR	External forward	*HSW*_F01	24	CTGTAAAACATAACACCTCCGTCG
		PCR	External reverse	*HSW*_R01	24	GTACTATGGCAACTCATTAAAGCC
	A. ochracea	PCR	External forward	*HSW*_F02	24	GCTGTAGCAAATAACTTTCCTTCG
		PCR	External reverse	*HSW*_R02	24	AAATATCAACCAGAACCCAATCCC
	C. hylas	PCR	External forward	*HSW*_F03	25	AGCGACTAGTAGTCGGACTACTCAC
		PCR	External reverse	*HSW*_R03	24	GCTTGTGAGACTATGATGATTTCC
	H. affinis	PCR	External forward	*HSW*_F04	23	TTAGTCGGACTACTCACTTCGTC
		PCR	External reverse	*HSW*_R04	24	CGCTTCAAGTTCTTTGAATATCCC
	N. himachala	PCR	External forward	*HSW*_F05	24	CAAGTGAGAAGCGACTTGTAGTCG
		PCR	External reverse	*HSW*_R05	24	TATTTCCTAAGAATGCGCGTCATG
	D. nerii	PCR	External forward	Same with *HSW*_F03		
		PCR	External reverse	*HSW*_R06	25	ACAACATCAAATGTCGCTCTATCTG
	M. pyrrhosticta	PCR	External forward	Same with *HSW*_F04		
		PCR	External reverse	*HSW*_R07	24	AAGGTAATTTTGGTATGGTGGGTG
	M. bombylans	PCR	External forward	Same with *HSW*_F03		
		PCR	External reverse	*HSW*_R08	24	CTTTTGTCTTCATCTCGTTACACG
	A. rubiginosa	PCR	External forward	*HSW*_F06	25	TCTGCGACTTGTAGTCGGACTACTC
		PCR	External reverse	*HSW*_R09	25	CTCCAATGACTTTGTAGCTGGTATG
	T. japonica	PCR	External forward	Same with *HSW*_F03		
		PCR	External reverse	*HSW*_R10	24	TGTGGGTAGAAGAGAATTGATTGG
	All	Sequencing	Internal forward	*HSW*_seqF01	18	GGGTTTCCTGACGACGTG
		Sequencing	Internal forward	*HSW*_seqF02	19	AGCGTTGAGATCAGGATAG
		Sequencing	Internall reverse	*HSW*_seqR01	20	ATCTTCTTGGCTTGCTCTTG
		Sequencing	Internall reverse	*HSW*_seqR02	19	GCCAGGTTTATCACGAACA
LW	*M. gaschkewitschii*	PCR	External forward	*HLW*_F01	25	GTAATAACCATCTCCAAGCGACTTC
		PCR	External reverse	*HLW*_R01	24	TAATAAAGAACATCGCTTCGGCAC
	A. ochracea	PCR	External forward	*HLW*_F02	23	CATCTCCAAGCGATTTCCCCTAC
		PCR	External reverse	*HLW*_R02	24	TAATAAAGAACATCGCTTCGGCAG
	C. hylas	PCR	External forward	*HLW*_F03	24	GTAATAACCATCTCAAAGCGACTC
		PCR	External reverse	Same with *HLW*_R02		
	H. affinis	PCR	External forward	Same with *HLW*_F03		
		PCR	External reverse	Same with *HLW*_R02		
	N. himachala	PCR	External forward	*HLW*_F04	24	CTACAGGAATTGTGTTGATACTCC
		PCR	External reverse	*HLW*_R03	24	GAACATCGCTTCGGCAAAATCGTG
	D. nerii	PCR	External forward	*HLW*_F05	22	TCTCCAAGCGACTCCCTTATCC
		PCR	External reverse	Same with *HLW*_R02		
	M. pyrrhosticta	PCR	External forward	*HLW*_F06	24	CATCTCTAAGCGATCCCTATCCTG
		PCR	External reverse	*HLW*_R04	24	TAATAAAGATCATCGCTTCGGCAG
	M. bombylans	PCR	External forward	Same with *HLW*_F06		
		PCR	External reverse	Same with *HLW*_R02		
	A. rubiginosa	PCR	External forward	Same with *HLW*_F05		
		PCR	External reverse	Same with *HLW*_R02		
	T. japonica	PCR	External forward	Same with *HLW*_F05		
		PCR	External reverse	Same with *HLW*_R02		
	All	Sequencing	Internal forward	*HLW*_seqF01	19	TGCCCGAAGGAAACATGAC
		Sequencing	Internal forward	*HLW*_seqF02	21	ACCATTTCCTTGTGGTTCATG
		Sequencing	Internall reverse	*HLW*_seqR01	20	TCATTTTCTTAGCCTGTTCC
		Sequencing	Internall reverse	*HLW*_seqR02	20	TAACAACCATAGCTGGAGAC

Analysis of opsin gene expression

For quantification of opsin gene expression, the RNA-seq reads were mapped to the three determined opsin cDNA sequences using the CLC genomics workbench 11.0.1 (https://www.qiagenbioinformatics.com/) for each individual. The reads per kilobase of exon model per million mapped reads (RPKM) were calculated to normalize the mRNA expression values (Mortazavi et al., 2008). I calculated the mean RPKM value with standard error (SE) from two or three individuals for each opsin gene, and compared the relative ratios between the three opsin genes in each species. The comparison of the RPKM values between nocturnal and diurnal species for each opsin gene was also assessed by the Wilcoxon rank-sum test using the package 'exactRankTests' (Hothorn and Hornik, 2019) in the R 3.3.3 program (R Core Team, 2017). $P < 0.05$ was considered a statistically significant difference.

Construction of opsin phylogenetic trees

In addition to the opsin sequences determined in the present study, I used three opsin sequences from *M. sexta*, *M. stellatarum* (GenBank accession nos.: UV; KF539456.1, SW; KF539426.1, LW; KF539444.1) and *H. armigera* (UV; KF539454.1, SW; KF539433.1, LW; KF539442.1) for construction of opsin gene trees. I aligned the sequences using CLUSTAL W (Thompson et al., 1994) in the MEGA v7.0 software (Kumar et al., 2016), followed by visual inspection (Figure 1A). Gene trees of orthologous opsin genes were also constructed by the ML method. The Jones-Taylor-Thornton (JTT)+G model for UV and SW opsins (Jones et al., 1992) and the Le and Gascuel 2008 (LG)+G model (Le and Gascuel, 2008) for LW opsin were selected as the best fit model of the amino acid substitution for the ML tree construction using the MEGA v7.0 software (Kumar et al., 2016). All positions containing gaps were removed from the alignment. The final data set contained 376 positions for UV opsin, 380 positions for SW opsin, and 377 positions for LW opsin. The statistical reliability of the tree branches was evaluated using 1,000 bootstrap replicates (Felsenstein, 1985). I used the FigTree v1.4.3 program (http://tree.bio.ed.ac.uk/software/figtree/) for the visualization of the

phylogenetic trees. I tested the ML gene tree topologies by comparing them to the topology of the hawkmoth species tree that I hypothesized to be the true gene tree topology, using the approximately unbiased (AU) test (Shimodaira, 2002) with 10,000 bootstrap replicates by the resampling estimated log-likelihood (RELL) method (Kishino et al., 1990) in the software IQ-TREE version 1.6.12 (Nguyen et al., 2015). The ML gene tree was considered to be significantly supported at the 95% level ($P \geq 0.95$).

To evaluate the positions of the amino acid replacements in the structure of opsin proteins, the seven transmembrane (TM) regions of each of the three opsin proteins for *M. sexta* as a representative of hawkmoths were predicted by the TMHMM-2.0 server (Sonnhammer et al., 1998; Krogh et al., 2001). By using the MEGA v7.0 software (Kumar et al., 2016), the amino acid sequences of three hawkmoth opsins were aligned with the rhodopsin-1 (Rh1, Kumopsin1; PDB accession no.: 6I9K_A) of a jumping spider (*Hasarius adansoni*) whose crystal structure has been published (Varma et al., 2019). The minimum distance between the retinal and each amino acid residue was examined based on the three-dimensional (3D) structure of jumping spider Rh1 using the iCn3D 2.10 viewer (Wang et al., 2020) in the Molecular Modeling Database (MMDB) (Madej et al., 2014). For visualization of the 3D structure of the protein, I executed the PyMOL Molecular Graphics System Version 2.3.0 (https://pymol.org). To confirm the homology between each gene sequence, I constructed the phylogenetic tree for all aligned opsins by the ML method under the LG amino acid substitution matrix with a gamma rate correction (Le and Gascuel, 2008). The tree construction and estimation of the best-fit substitution model were conducted by the MEGA v7.0 software (Kumar et al., 2016). The final dataset included a total of 486 positions. The reliability of the tree topology was evaluated by bootstrap analysis with 1,000 replications (Felsenstein, 1985). For visualization of the tree, I executed the FigTree v1.4.3 program (http://tree.bio.ed.ac.uk/software/figtree/) (Figure. 1B). Throughout the paper, the amino acid residue numbers were based on those of each opsin in *M. sexta*.


A
Bovine rhodopsin
Squid rhodopsin
Jumping spider Rh1
H. armigera LW
M. gaschkewitschii LW
A. ochracea LW
M. sexta LW (Manop1)
C. hylas LW
H. affinis LW
N. himachala LW
D. nerii LW
M. pyrrhosticta LW
M. bombylans LW
M. stellatarum LW
A. rubiginosa LW
T. japonica LW
H. armigera UV
M. gaschkewitschii SW
A. ochracea SW
M. sexta SW (Manop3)
C. hylas SW-A
C. hylas SW-B
H. affinis SW-A
H. affinis SW-B
N. himachala SW
D. nerii SW
M. pyrrhosticta SW
M. bombylans SW
M. stellatarum SW
A. rubiginosa SW
T. japonica SW
A. ochracea UV-A
A. ochracea UV-B
M. sexta UV (Manop2)
C. hylas UV
H. affinis UV
N. himachala UV
D. nerii UV
M. pyrrhosticta UV
M. bombylans UV
M. stellatarum UV
A. rubiginosa UV
T. japonica UV

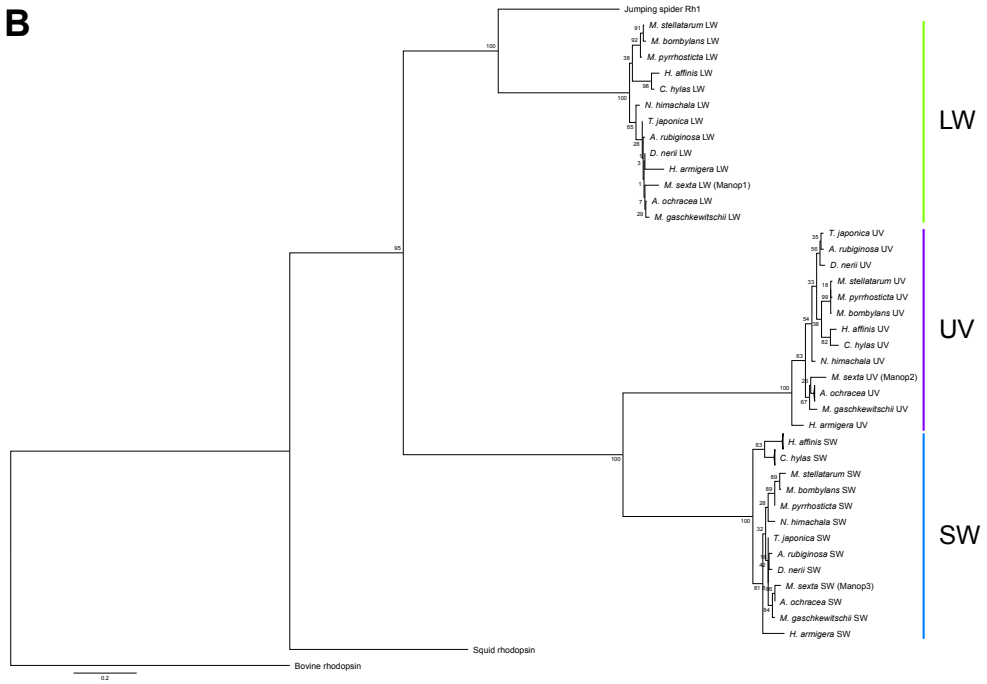

Figure 1. Sequence relatedness among the opsin genes. (A) Alignment for the amino acid sequences of the opsins. Seven putative membrane spanning domains are highlighted in gray. Dots indicate the identical residues to those of the top line and dashes represent sequence gaps. (B) On the basis of the amino acid alignment, the phylogenetic tree of the opsins was reconstructed by the ML method. Bootstrap values with 1,000 replicates are shown at the nodes. Scale bar indicates 0.2 amino acid substitutions per site. The branches of the polymorphisms are collapsed. Moth visual opsin genes clustered into three groups: UV, SW, and LW opsins.

Comparison of dN/dS (ω) of opsin genes

To elucidate whether the evolutionary rates of amino acid substitution changed between the nocturnal and diurnal branches, I performed ML calculations to estimate synonymous (dS) and non-synonymous (dN) substitution rates, and their ratio (dN/dS = ω), for the three opsin genes in the 12 hawkmoth species. I considered two models: the simplest model assuming the same ω value across the tree (one-ratio model), and the model allowing variable ω values between nocturnal and diurnal branches (two-ratio model). The simpler one-ratio model was nested in the two-ratio model. The likelihoods of the former and latter models were compared to test whether the ratio for diurnal branches was the same as the ratio for nocturnal ones. Log-likelihood (lnL) and ω at branches were calculated by the branch model using the program codeml in the PAML 4.8a package (Yang, 1997, 2007) with PAMLX 1.3.1 (Xu and Yang, 2013). The fit of branch models was assessed using the likelihood ratio test (LRT) by χ^2 test to the 2 × (log-likelihood difference) (2 ΔlnL), with the one-ratio model rejected where $P < 0.05$. I used the alignments of the opsin cDNA nucleotide sequences from which indels were removed. The analysis was performed based on the topology of the hawkmoth species tree presented in this study. *M. stellatarum*, which was not included in the species tree, was combined to form a cluster with *M. bombylans* because *M. stellatarum* and *M. bombylans* were monophyletic in the three opsin phylogenetic trees. The branches forming the monophyletic groups of diurnal species were defined as diurnal branches.

Statistical test for parallel evolution of opsin amino acid sequences

First, I searched for the opsin amino acid substitutions that occurred in parallel in the three different diurnal clades. For the three opsins, I reconstructed the ancestral states at the nodes by the ML method (Nei and Kumar, 2000) under the JTT matrix-based model with a gamma distribution for rates among sites (Jones et al., 1992), which was chosen as the best fit model using the MEGA v7.0 software (Kumar et al., 2016). The analysis was performed based on the topology of the hawkmoth species tree presented in this study. I identified the parallel-substitution sites between the three independent diurnal

lineages according to the definition of Zhang and Kumar (1997).

Next, I analyzed whether the parallel substitutions of amino acids occurred by chance or not. I used the hawkmoth opsin amino acid sequences and the species tree topology, and obtained the assigned notation of the nodes using the program ancestor in the ANCESTOR package (Zhang and Nei, 1997). Two focused diurnal lineages in the different clades were selected for the statistical tests of parallel evolution of amino acid sequences. When the focused clade contained more than one diurnal species, one sequence was used for the analysis. I counted the total number of parallel-substitution sites on the lineage from the interior nodes, where the common ancestor of the diurnal species diverged from the nocturnal species, to the exterior nodes of the tree for the lineage pair. I performed a Poisson test to verify whether the observed number of parallel substitutions was significantly larger than the expected number due to random substitution under the JTT-f_{gene} amino acid substitution model (Cao et al., 1994) using the program converg2 in the CAPE package (Zhang and Kumar, 1997). At a significance level of $P = 0.05$, I rejected the null hypothesis that the observed parallel substitutions were simply attributed to random chance.

Electrophysiology of compound eye spectral sensitivity

To examine the absorption spectra of visual pigments, I determined the compound eyes' spectral sensitivities in the four hawkmoth species by recording the electroretinograms (ERGs). Under dim red light, I fixed a moth onto a plastic stage with beeswax. I inserted a chloridized silver wire into the stump of an antenna to serve as the reference electrode. After making a tiny crack on the cornea with a razor blade, I mounted the sample in a Faraday cage covered with a blackout curtain. I then inserted the tip of a glass microelectrode filled with physiological saline into the eye through the crack using a micromanipulator. An end-of-quartz optical fiber (Φ3) for light stimulation was placed close to the eye, and its position was fine-tuned to maximize the responses to dim flashes. Before recording the ERG, the sample was left in the dark for at least 2 hrs in the nocturnal species and at least 30 min in the diurnal species so that the eye was dark-adapted.

The light was provided by a 500 W xenon arc lamp (UXL-500D-O, Ushio Inc., Tokyo, Japan) through a series of 23 narrow-band interference filters ranging from 300 to 740 nm at 20 nm intervals (full width at half maximum, FWHM = 10–14 nm, Asahi Spectra, Tokyo, Japan). Light intensity was controlled by a set of neutral density (ND) filters. The photon flux of each monochromatic light was measured using a radiometer (Model-470D, Sanso, Tokyo, Japan) and attenuated to equal density (5.0×10^{11} photons per square centimeter per sec) at the corneal surface using an optical wedge. The ERG responses were recorded through a biophysical amplifier (AVB-10, Nihon Kohden, Tokyo, Japan) with a high-impedance probe (JB-101J, Nihon Kohden) connected to a computer with the AcqKnowledge 3.9.1.6 software (BIOPAC Systems, Goleta, CA, USA) via an analogue-to-digital (A/D) converter (MP-150, BIOPAC Systems).

I stimulated the dark-adapted eye with a series of monochromatic flashes of 200 msec duration, separated by 15 sec intervals, to record spectral response. The wavelength first varied from short to long wavelengths and then in the reverse order. The pairs of bidirectional stimulation were recorded at least twice. I then measured the responses to light of varying intensities over a 4 log-unit at the wavelength that gave the maximum response. The response amplitude-log intensity (V-log I) data were fitted to the Naka-Rushton function:

$$\frac{V}{V_{\max}} = \frac{I^n}{I^n + K^n}, \tag{1}$$

where I is the stimulus intensity, V is the response amplitude, $V_{\max}$ is the maximum response amplitude, K is the stimulus intensity eliciting 50% of $V_{\max}$, and n is the exponential slope (Naka and Rushton, 1966), using the custom-made programs implemented in MATLAB R2018a (The MathWorks, Inc., Natick, Massachusetts, USA). The sensitivity is defined as the reciprocal of the stimulus intensity I required for a criterion response (Menzel, 1979). Based on the obtained sigmoidal V-log I function, I converted the spectral response into the spectral sensitivity, $S(\lambda)$, and normalized it to the maximum sensitivity. I calculated the $S(\lambda)$ of each individual by averaging the 2–4 paired spectral series from the ERG-recording in one sample, and then determined the $S(\lambda) \pm$ SE for each species by averaging those of the multiple individuals.

Estimation of visual pigment absorption spectra

I assumed that the hawkmoth ERG-determined $S(\lambda)$ could be modelled as a weighted sum of the absorption spectra of UV, SW, and LW-absorbing visual pigments (Satoh et al., 2017). According to Stavenga et al. (1993) and Stavenga (2010), the absorbance spectrum of the visual pigments, $R_i(\lambda)$, is assumed as the summation of the α- and β-absorbance bands:

$$R_i(\lambda) = \sum_j p_j \alpha_{ij}(\lambda), \quad (2)$$

where i = UV, SW, LW, j = α-band, β-band, λ is the wavelength, and p_j is the relative amplitude. $\alpha_{ij}(\lambda)$ is the absorbance of each band, which is described by:

$$\alpha_{ij}(\lambda) = \exp\left\{-a_j x^2 \left[1 + b_j x + \frac{3}{8}(b_j x)^2\right]\right\}, \quad (3)$$

with

$$x = \log_{10}\left(\frac{\lambda}{\lambda_{\max,ij}}\right), \quad (4)$$

where $\lambda_{\max,ij}$ is the peak wavelength (Stavenga et al., 1993). The parameter values are as follows: $p_{\beta\text{-band}} / p_{\alpha\text{-band}} = 0.29$, $a_{\alpha\text{-band}} = 380$, $b_{\alpha\text{-band}} = 6.09$, $a_{\beta\text{-band}} = 247$, $b_{\beta\text{-band}} = 3.59$ (Stavenga et al., 1993). I fixed the $\lambda_{\max}$ of the β-band at 360 nm according to the previous fitting in the butterfly photoreceptors (Arikawa et al., 1999).

The simplest case of ERG-determined $S(\lambda)$ with three visual pigments can be modelled as a weighted sum of the template absorbance spectra:

$$S(\lambda) = \sum_i f_i R_i(\lambda), \quad (5)$$

where f_i is the relative contribution. I estimated the parameters $\lambda_{\max}$ and f_i by the model fittings using the nonlinear least-squares algorithm *nlsLM* from the package 'minpack.lm' (Elzhov et al., 2016) in the R 3.3.3 program (R Core Team, 2017).

Satoh et al. (2017) measured and modelled the absorbance spectra of the screening pigments in the summer fruit tortrix moth, *Adoxophyes orana*. Following their procedure, I modelled the screening pigments' absorbance spectrum $A(\lambda)$ with a sum of two Gaussian functions:

$$A(\lambda) = p_1 \exp\left[\frac{-(\lambda-\mu_1)^2}{2\sigma_1^2}\right] + p_2 \exp\left[\frac{-(\lambda-\mu_2)^2}{2\sigma_2^2}\right], \quad (6)$$

where μ_1 and μ_2 are the peak wavelengths, σ_1 and σ_2 are the standard deviations (SD), and p_1 and p_2 are the relative contributions, respectively. I incorporated $A(\lambda)$ in equation 5 to estimate the λ_{max} values with the effect of the screening pigments taken into account. The resulting spectral sensitivity $S_a(\lambda)$ is:

$$S_a(\lambda) = S(\lambda) - A(\lambda). \quad (7)$$

I estimated the parameters $\lambda_{max}, f_i, \mu_1, \mu_2, \sigma_1, \sigma_2, p_1$ and p_2 using the nonlinear least-squares algorithm *nlsLM* from the package 'minpack.lm' (Elzhov et al., 2016) in the R 3.3.3 program (R Core Team, 2017).

Histology of compound eye

For anatomy, I used males of the same four species with which I did electrophysiology. The eyes were light-adapted for 30 min under room light. The light-adapted eyes were dissected under a dissection microscope and prefixed in 2% paraformaldehyde and 2.5% glutaraldehyde in 0.1M sodium cacodylate buffer at pH 7.4 (CB) for 30–60 min at room temperature. After being washed with 0.2M CB, the eyes were dehydrated through an acetone series, infiltrated with propylene oxide, and embedded in Epon. I cut 10 μm thick sections with a rotatory microtome (HM 355 S, MICROM GmbH, Walldorf, Germany) and observed the sections under a light microscope (BX60, Olympus Optical Co., LTD, Tokyo, Japan) without staining.

Chapter 4. Results

Three independent emergences of diurnal lineages in hawkmoths

I constructed a Maximum Likelihood (ML) tree based on the RNA-seq short-read sequences to investigate the phylogeny of hawkmoth species (Figure 2). The phylogenetic tree inferred from 17,305 informative positions representing the whole genome can be considered as a hawkmoth species tree. All branches were supported by high bootstrap values (97–100), except for one. The phylogenetic relationship was almost the same as the one proposed in a previous study based on five nuclear loci (Kawahara et al., 2009). I estimated the emergence of diurnal species/lineages based on the species tree, assuming that diurnal species diverged from the nocturnal ancestors and the evolution in the opposite direction did not occur because most species/lineages of hawkmoths are nocturnal and the nocturnal niche has been already occupied by ancestral hawkmoth species. As shown in Figure 2, the basal lineage of hawkmoth species was nocturnal, which has been suggested by Kawahara et al., (2009). The diurnal species/lineages independently appeared three times: the *C. hylas/H. affinis*, *N. himachala*, and *M. pyrrhosticta/M. bombylans* lineages, named as D1, D2, and D3, respectively (D1–3 in Figure 2).

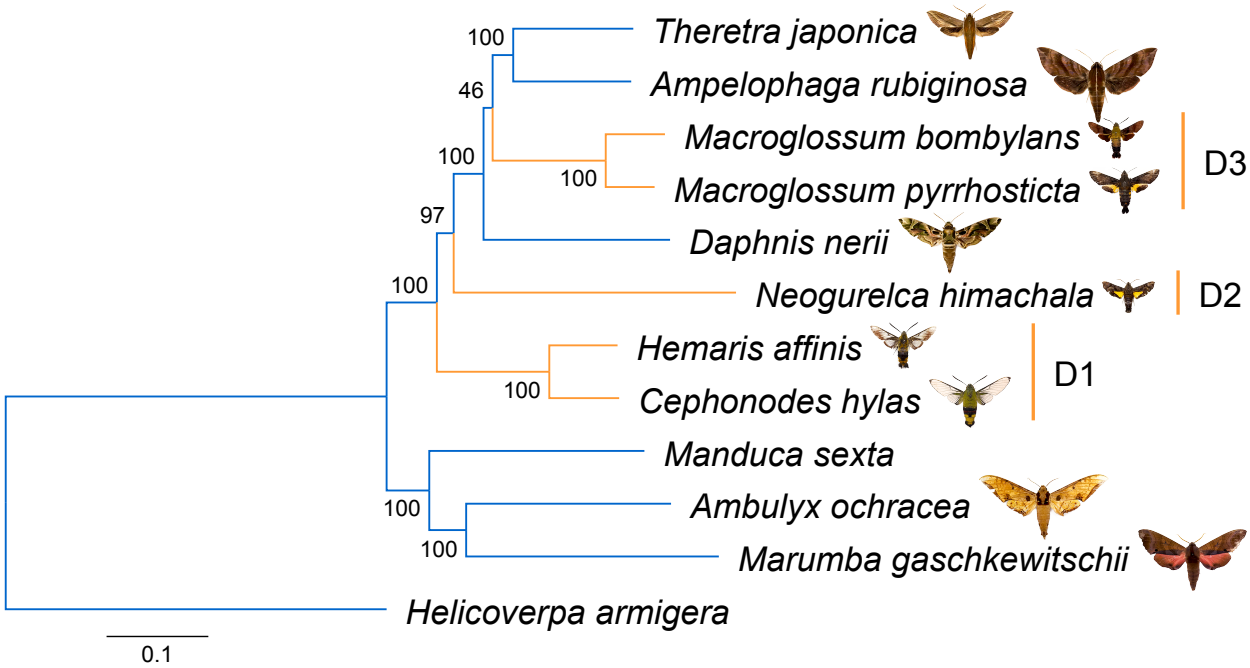

Figure 2. Phylogenetic tree of hawkmoth. A ML tree for hawkmoth species (Sphingidae) constructed by assembled, aligned and concatenated RNA-seq reads. *H. armigera* was used as an outgroup species. Scale bar indicates 0.1 nucleotide substitutions per site. The bootstrap values are shown at the nodes. The indigo branches are nocturnal, and the orange branches are diurnal. D1–3 represent the diurnal clades. Photographs of the hawkmoths collected in this study are at the same magnification.

Expression of opsin genes

I assembled the transcriptomes which consistently contained 85.3–94.7% of complete and fragmented BUSCOs, and identified three visual opsin genes (*UV*, *SW* and *LW*) in the transcriptomes of all ten hawkmoth species. Subsequently, I assembled both ends of the coding regions with UTRs and verified the full-length cDNA sequences by PCR and sequencing.

I then performed expression analysis for the three opsin genes in the ten species (Figure 3). The relative expression ratios were 1.8–9.2% in *UV*, 4.4–14.6% in *SW*, and 79.3–93.8% in *LW* genes. The relative expression levels of the *SW* gene appeared to be slightly higher than that of the *UV* gene, but the order was opposite in *H. affinis* (Figure 3). These results suggest that the *LW* gene is predominantly expressed, while the *UV* and *SW* genes are expressed almost equally in hawkmoth eyes.

I compared the RPKM values of these genes between the nocturnal and diurnal species, and found no significant differences in the expression values between the nocturnal and diurnal species for all the three opsin genes ($P > 0.15$, in every case; Figure 4). The distributions of mRNA expression levels rather tended to reflect the closeness in the phylogeny of hawkmoths (Figure 4).

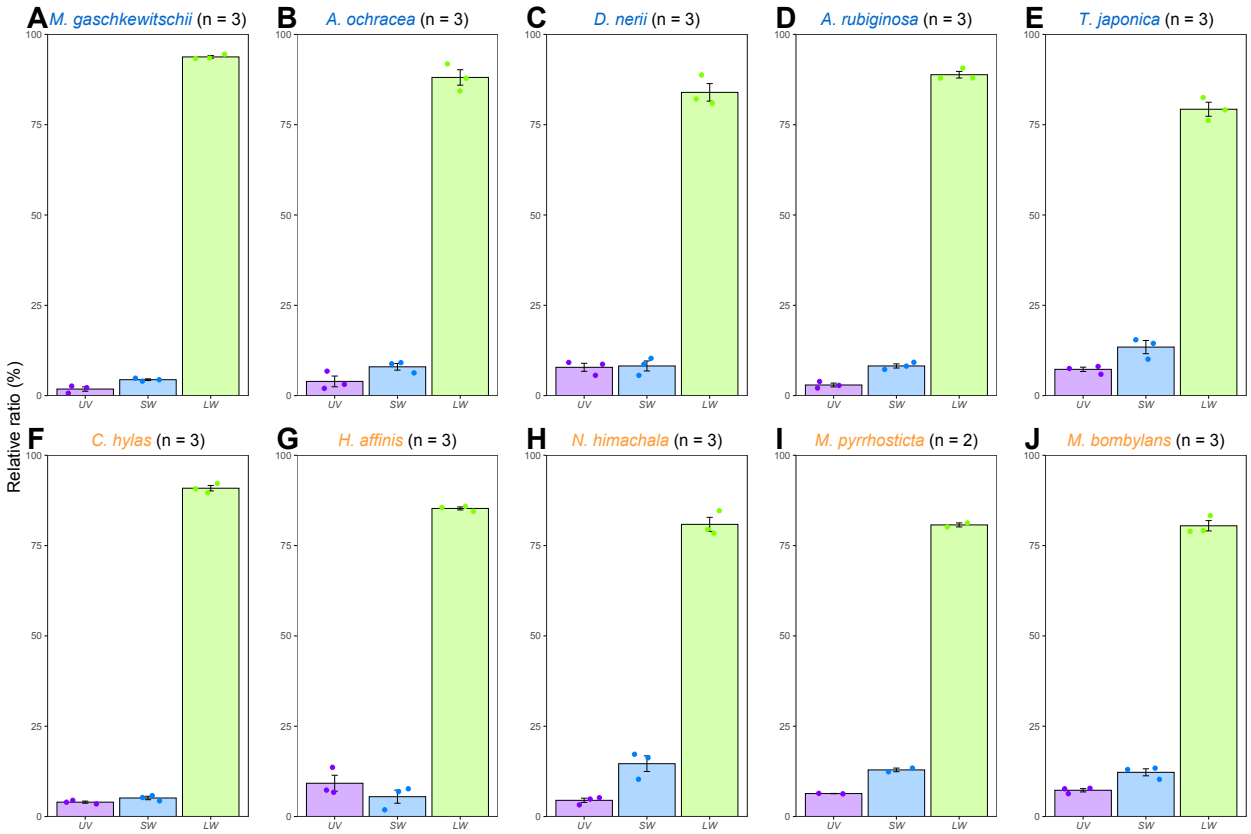

Figure 3. Relative expression ratios of the three opsin genes. Relative expression ratios, mean ± SE, of mRNAs encoding the three opsins in the (A–E) nocturnal species and (F–J) diurnal species were quantified based on the RPKM values. One dot represents the ratio in one individual, and the number of individuals, n, is shown next to the species name.

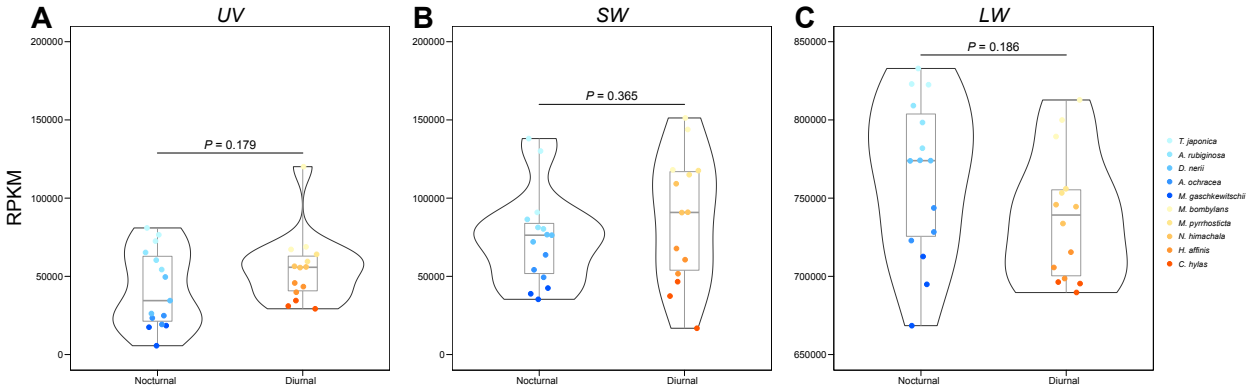

Figure 4. Comparison of the distributions of RPKM values of opsin genes between the nocturnal and diurnal species. The violin plots show the distributions of the RNA-seq RPKM values of (A) *UV*, (B) *SW*, or (C) *LW* opsins for the nocturnal and diurnal species. The thick middle lines in the inner boxes indicate the medians, the tops and bottoms of the boxes indicate the third and the first quartiles, respectively, and the lower and upper error bars indicate the minimum and the maximum values. One dot denotes one individual, and differently colored dots represent different species according to the marginal note. The Wilcoxon rank sum test was performed, and no significant differences were shown between the nocturnal and diurnal species for all the three opsins.

Parallel evolution of opsin genes in diurnal lineages

Figure 5 shows the ML gene trees of the three opsin genes. The topology of the UV opsin tree (Figure 5A) reflects the species' phylogenetic relationships (Figure 2). In contrast, the SW and LW opsin trees exhibit distinct branching patterns from the species tree: SW and LW opsins in diurnal species form monophyletic groups in both trees (Figure 5B,C). In the AU test comparing the ML gene tree to the gene tree with the species tree topology, the ML tree of UV opsin was not significantly different from the other ($P = 0.69$), whereas the ML trees of SW and LW opsins were significantly supported ($P = 0.99$ and $P = 0.99$, respectively). These results indicate that the parallel amino acid substitutions may have occurred on the diurnal branches under selective pressure different from those on the nocturnal branches (Kreitman and Akashi, 1995; Adachi and Hasegawa, 1996). Therefore, I first estimated and compared the dN/dS ratio (ω value) to ascertain whether the amino acid substitutions have accelerated in the diurnal branches.

The ω values of the branches are < 1 in all the opsins, which means that the three visual opsin genes have evolved under negative (purifying) selection with functional constraints on the entire gene throughout their evolution (one-ratio model; Table 3). However, I found that the ω values of the diurnal branches were significantly higher than those of the nocturnal branches in all three opsins ($P < 0.05$, two-ratio model; Table 3). In the branch model comparison, if the ω value on the foreground diurnal branch is higher than that on the background nocturnal branch but not higher than 1, the result is not sufficient to support that positive selection has acted on the gene. Then, I extended the analysis to see whether non-neutral parallel evolution has occurred on the diurnal opsin genes.

I inferred the ancestral amino acid sequences at each node, and identified the parallel amino acid substitutions in at least two of the three diurnal lineages (D1–3 in Figure 6). The total numbers of amino acid substitutions which occurred in parallel were 8 for UV opsin, 16 for SW opsin, and 21 for LW opsin (Figures 6 and 7, Table 4). I also identified one parallel deletion (ΔP372) in two diurnal branches, D2 and D3, of UV opsin (Figures 6A and 7A). A pairwise statistical analysis was then performed to compare the number of parallel amino acid substitutions with the expected number

which would occur by chance under neutral evolution. For SW and LW opsins, the numbers of parallel substitutions observed in all 11 pairs of diurnal lineages were significantly larger than expected ($P < 0.05$, Table 4). The observed numbers for UV opsin were significantly larger than expected in 8 of the 11 pairs of diurnal lineages ($P < 0.05$, in those cases; Table 4).

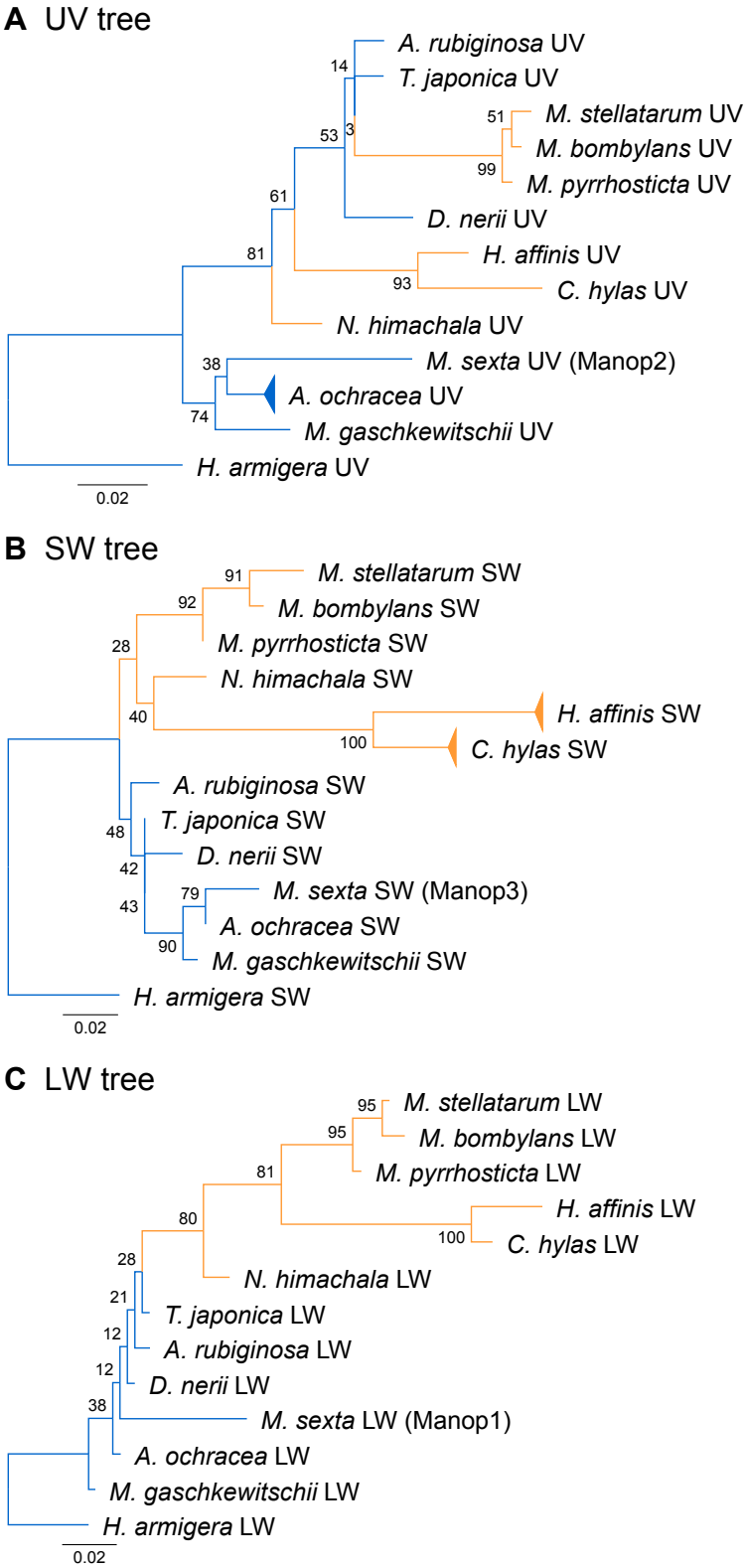

Figure 5. Phylogenetic trees of opsins. (A) UV, (B) SW, and (C) LW opsins gene trees constructed by the ML method. Each orthologous opsin of *H. armigera* was used as an outgroup. The polymorphic branches are collapsed. Scale bar indicates 0.02 amino acid substitutions per site. The bootstrap values are shown at the nodes. The indigo branches are nocturnal, and the orange branches are diurnal.

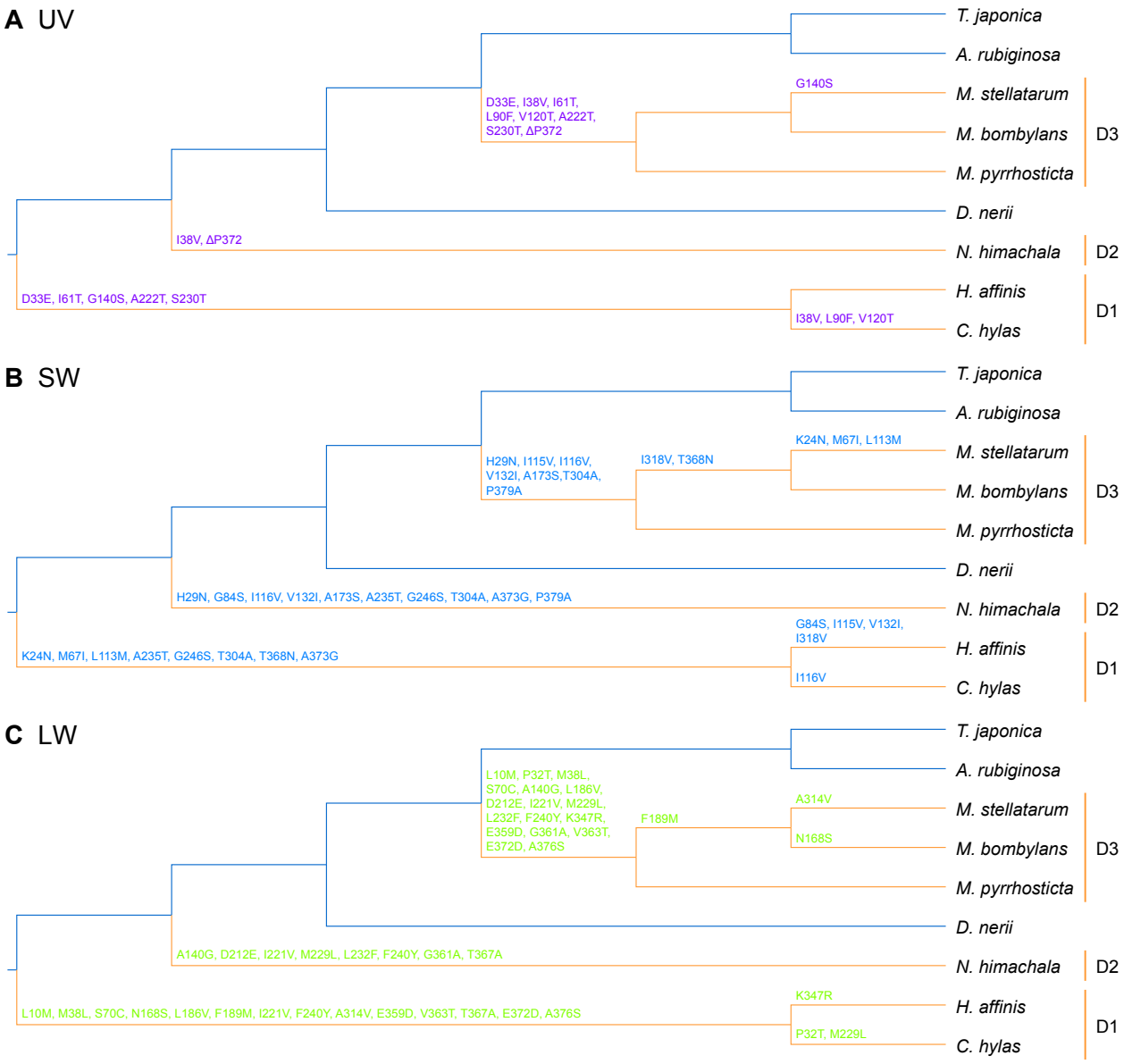

Figure 6. Parallel amino acid substitutions of the opsins on the diurnal branches. The tree topology is based on the phylogenetic tree of hawkmoth species (Figure 2). The *M. stellatarum* branch is joined with the *M. bombylans* branch on the basis of the three opsin gene trees (Figure 5). The parallel amino acid substitutions in (A) UV, (B) SW, and (C) LW opsins among the diurnal species/lineages are shown on the branches. The indigo branches are nocturnal, and the orange branches are diurnal. D1–3 represent diurnal clades. The amino acid residue numbers follow those of each orthologous opsin in *M. sexta*.

A UV

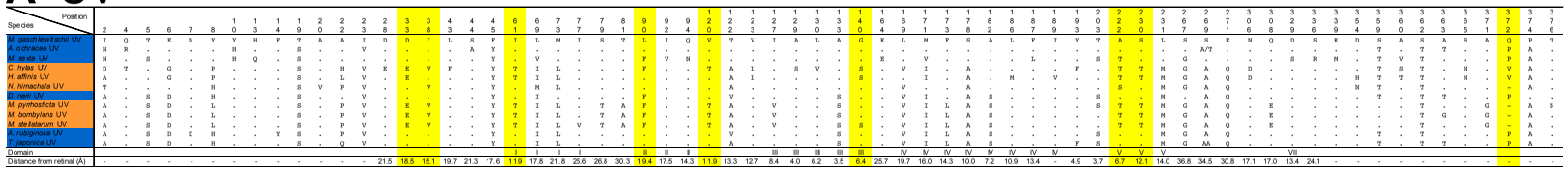
Position
Species
M. gaschkewitschii UV
A. pyhracea UV
M. setia UV
C. hyas UV
H. affinis UV
N. himachala UV
D. nelli UV
M. pyrrhosticta UV
M. bombylans UV
M. stetaramum UV
A. fuliginosa UV
T. japonica UV
Domain
Distance from retinal (Å)

B SW

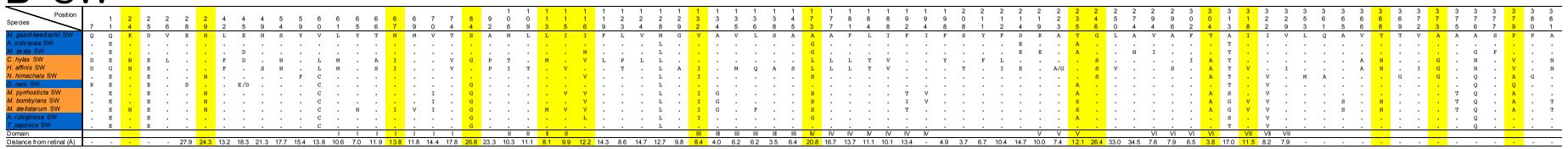
Position
Species
M. gaschkewitschii SW
A. pyhracea SW
M. setia SW
C. hyas SW
H. affinis SW
N. himachala SW
D. nelli SW
M. pyrrhosticta SW
M. bombylans SW
M. stetaramum SW
A. fuliginosa SW
T. japonica SW
Domain
Distance from retinal (Å)

C LW

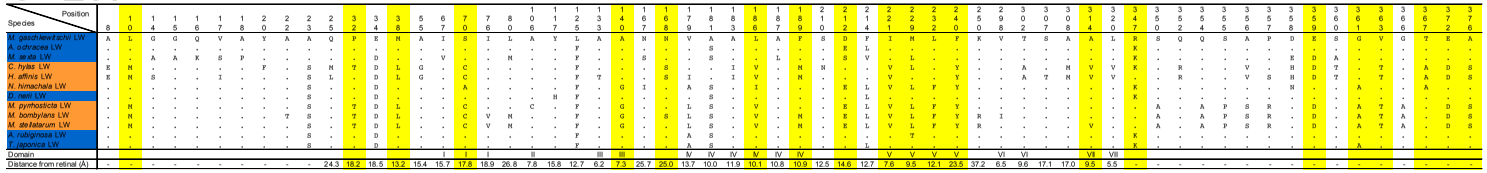
Position
Species
M. gaschkewitschii LW
A. pyhracea LW
M. setia LW
C. hyas LW
H. affinis LW
N. himachala LW
D. nelli LW
M. pyrrhosticta LW
M. bombylans LW
M. stetaramum LW
A. fuliginosa LW
T. japonica LW
Domain
Distance from retinal (Å)

Figure 7. Amino acid alignments of the informative positions for the three opsins. In (A) UV, (B) SW, and (C) LW opsins, the parallel substitutions occurring in the diurnal species/lineages are highlighted in yellow. The amino acid positions follow those of each orthologous opsin in *M. sexta*. Dots indicate identical residues to those of the top line. TM domains were deduced based on each orthologous opsin sequence of *M. sexta,* and the minimum distances between the retinal and the amino acid positions were estimated based on the 3D structure of jumping spider Rh1.

Table 3. Likelihood ratio tests for branch model comparison of the hawkmoth opsins

	One-ratio model			Two-ratio model			Likelihood ratio test		
Opsin	ω	lnL	np	ω1 (nocturnal); ω2 (diurnal)	lnL	np	2 Δ lnL	d.f.	*P*
UV	0.041	-5209.29	23	0.032; 0.060	-5204.18	24	10.225	1	$\mathbf{1.4^{-3}}$
SW	0.043	-5347.59	23	0.015; 0.088	-5309.39	24	76.401	1	$\mathbf{2.3^{-18}}$
LW	0.058	-4728.38	23	0.026; 0.101	-4708.52	24	39.717	1	$\mathbf{2.9^{-10}}$

lnL, log-likelihood; np, number of parameters; ω, non-synonymous/synonymous rate ratio (dN/dS)

Table 4. Tests for parallel evolution of the opsin sequences of the diurnal hawkmoth species

Opsin (length)	Lineage pair	Observed no. of parallel substitutions (site positions)	Expected no. of parallel substitutions	*P*
UV (376 aa)	*C. hylas–N. himachala*	1 (38)	0.066	0.064
	C. hylas–M. pyrrhosticta	7 (33, 38, 61, 90, 120, 222, 230)	0.135	**1.5^{-10}**
	C. hylas–M. bombylans	7 (33, 38, 61, 90, 120, 222, 230)	0.134	**1.4^{-10}**
	C. hylas–M. stellatarum	8 (33, 38, 61, 90, 120, 140, 222, 230)	0.144	**4.1^{-12}**
	H. affinis–N. himachala	0	0.047	1.000
	H. affinis–M. pyrrhosticta	4 (33, 61, 222, 230)	0.105	**4.6^{-6}**
	H. affinis–M. bombylans	4 (33, 61, 222, 230)	0.104	**4.5^{-6}**
	H. affinis–M. stellatarum	5 (33 ,61, 140, 222, 230)	0.111	**1.3^{-7}**
	N. himachala–M. pyrrhosticta	1 (38)	0.050	**0.048**
	N. himachala–M. bombylans	1 (38)	0.049	**0.048**
	N. himachala–M. stellatarum	1 (38)	0.054	0.053
SW (383 aa)	*C. hylas–N. himachala*	5 (116, 235, 246, 304, 373)	0.158	**7.1^{-7}**
	C. hylas–M. pyrrhosticta	2 (116, 304)	0.173	**0.013**
	C. hylas–M. bombylans	3 (116, 304, 368)	0.228	**1.7^{-3}**
	C. hylas–M. stellatarum	6 (24, 67, 113, 116, 304, 368)	0.315	**1.0^{-6}**
	H. affinis–N. himachala	6 (84, 132, 235, 246, 304, 373)	0.193	**6.1^{-8}**
	H. affinis–M. pyrrhosticta	3 (115, 132, 304)	0.215	**1.4^{-3}**
	H. affinis–M. bombylans	5 (115, 132, 304, 318, 368)	0.286	**1.3^{-5}**
	H. affinis–M. stellatarum	8 (24, 67, 113, 115, 132, 304, 318, 368)	0.388	**9.1^{-9}**
	N. himachala–M. pyrrhosticta	6 (29, 116, 132, 173, 304, 379)	0.054	**3.2^{-11}**
	N. himachala–M. bombylans	6 (29, 116, 132, 173, 304, 379)	0.072	**1.8^{-10}**
	N. himachala–M. stellatarum	6 (29, 116, 132, 173, 304, 379)	0.101	**1.4^{-9}**
LW (377 aa)	*C. hylas–N. himachala*	4 (221, 229, 240, 367)	0.104	**4.5^{-6}**
	C. hylas–M. pyrrhosticta	12 (10, 32, 38, 70, 186, 221, 229, 240, 359, 363, 372, 376)	0.276	**4.4^{-16}**
	C. hylas–M. bombylans	14 (10, 32, 38, 70, 168, 186, 189, 221, 229, 240, 359, 363, 372, 376)	0.343	**1.1^{-16}**
	C. hylas–M. stellatarum	14 (10, 32, 38, 70, 186, 189, 221, 229, 240, 314, 359, 363, 372, 376)	0.319	**1.1^{-16}**
	H. affinis–N. himachala	3 (221, 240, 367)	0.118	**2.5^{-4}**
	H. affinis–M. pyrrhosticta	11 (10, 38, 70, 186, 221, 240, 347, 359, 363, 372, 376)	0.303	**3.8^{-14}**
	H. affinis–M. bombylans	13 (10, 38, 70, 168, 186, 189, 221, 240, 347, 359, 363, 372, 376)	0.378	**5.6^{-16}**
	H. affinis–M. stellatarum	13 (10, 38, 70, 186, 189, 221, 240, 314, 347, 359, 363, 372, 376)	0.351	**1.1^{-16}**
	N. himachala–M. pyrrhosticta	7 (140, 212, 221, 229, 232, 240, 361)	0.090	**8.8^{-12}**
	N. himachala–M. bombylans	7 (140, 212, 221, 229, 232, 240, 361)	0.119	**6.1^{-11}**
	N. himachala–M. stellatarum	7 (140, 212, 221, 229, 232, 240, 361)	0.108	**3.2^{-11}**

Absorption spectra of visual pigments

To assess the absorption spectra of the three visual pigments, I measured the eye's spectral sensitivity, $S(\lambda)$, by recording ERG responses to monochromatic lights. Figure 8 shows the $S(\lambda)$ of the dark-adapted hawkmoths (filled circles with error bars). All spectra exhibit peaks in the UV and green wavelength regions, typical in many insects including moths (Wakakuwa et al., 2014; Satoh et al., 2017). The dotted colored lines in each panel represent the predicted absorption spectra of UV, SW, and LW pigments multiplied by the contribution factors (f_i in equation 5). The contribution of LW pigments is equally high in all the species. The solid black line is the summation of these three spectra.

I revealed that the predicted absorption spectra of SW and LW pigments differed between the nocturnal and diurnal species. Table 5 summarizes the estimated λ_{max} and f_i values. In the diurnal species, the λ_{max} values of SW pigments shifted about 10 nm on average to the long-wavelength direction: 16.0 nm shift for *C. hylas* and 5.0 nm shift for *M. pyrrhosticta* from the average value of nocturnal species, respectively. On the other hand, the shift direction was opposite in LW pigments, i.e., the λ_{max} values were about 10 nm shorter in diurnal species: 14.7 nm shift for *C. hylas* and 5.8 nm shift for *M. pyrrhosticta* from the average value of nocturnal species, respectively. Meanwhile, the λ_{max} values of UV pigments were similar.

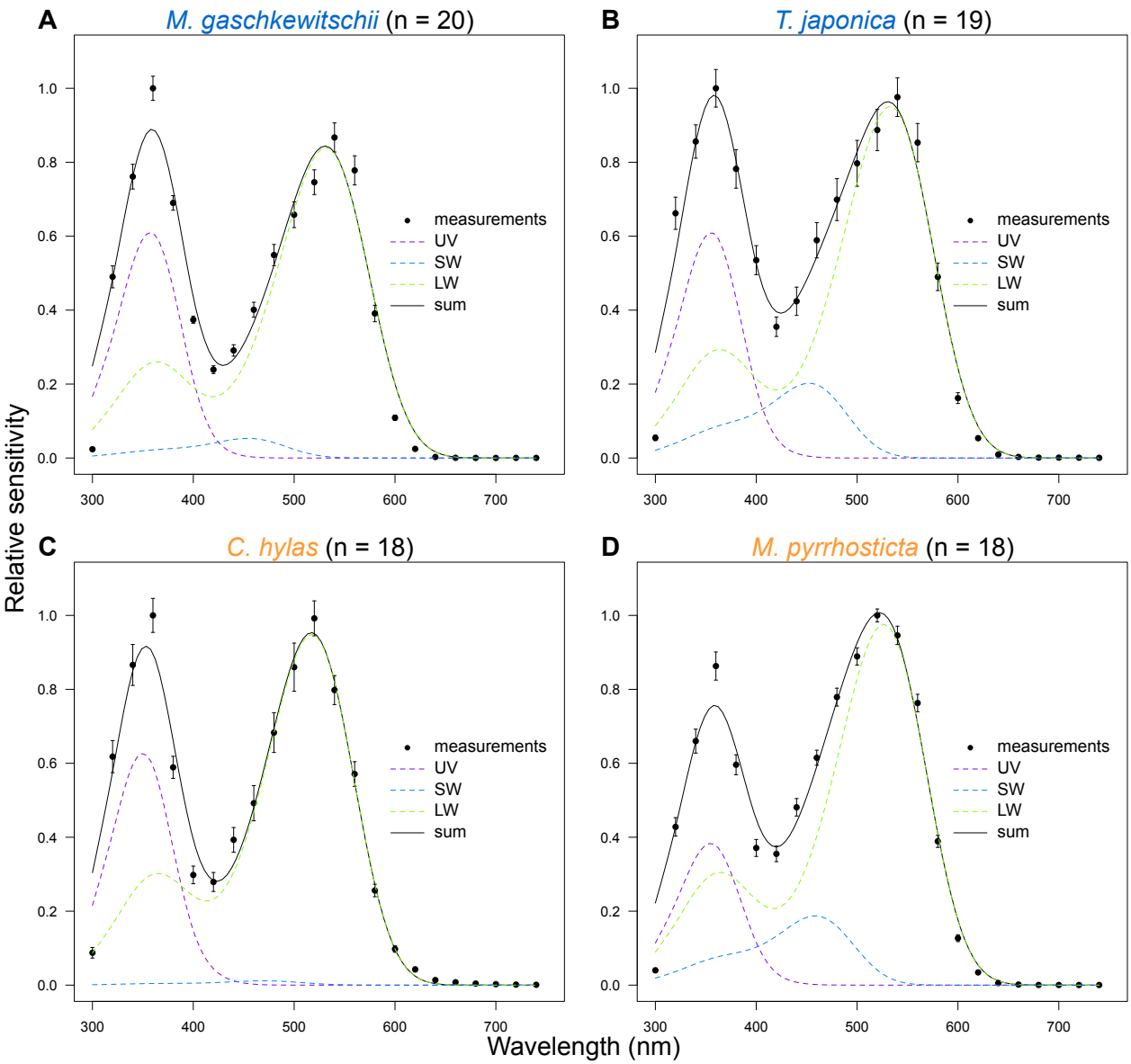

Figure 8. Spectral sensitivities of the compound eyes determined by ERG and the estimated visual pigments' absorption spectra. In the (A, B) nocturnal and (C, D) diurnal species, filled circles indicate mean ± SE of the measurements in multiple individuals, n, shown next to the species name. Dotted color lines are the absorption spectra of the individual visual pigments, and the solid black line is the weighted sum of the three spectra.

Table 5. Estimated parameters of the absorption spectra of visual pigments in the hawkmoth species

Species	UV λ_{max} (nm)	Mean ($\Delta\lambda_{max}$ from Noct.) (nm)	SW λ_{max} (nm)	Mean ($\Delta\lambda_{max}$ from Noct.) (nm)	LW λ_{max} (nm)	Mean ($\Delta\lambda_{max}$ from Noct.) (nm)	UV amplitude f_{UV} (relative ratio, %)	SW amplitude f_{SW} (relative ratio, %)	LW amplitude f_{LW} (relative ratio, %)
M. gaschkewitschi (n = 20)	357.0	355.8	455.0	454.2	531.4	532.1	0.473 (34.6%)	0.053 (3.9%)	0.840 (61.5%)
T. japonica (n = 19)	354.5		453.3		532.8		0.474 (29.2%)	0.201 (12.3%)	0.951 (58.5%)
C. hylas (n = 18)	348.2	351.0 (-4.8)	470.1	464.6 (+10.4)	517.4	521.9 (-10.2)	0.491 (33.8%)	0.012 (0.8%)	0.948 (65.4%)
M. pyrrhosticta (n = 18)	353.7		459.1		526.3		0.298 (20.4%)	0.186 (12.8%)	0.976 (66.8%)

Chapter 5. Discussion

Driving force for parallel evolution of diurnal opsin sequences

In this study, I constructed a phylogenetic tree of hawkmoth species and the diurnal lineages of hawkmoths independently appeared at least three times in the subfamily Macroglossinae after hawkmoth divergence around 42.8 MYA before subtribe Choerocampina divergence around 12.2 MYA (Kawahara et al., 2019). Opsin gene duplications and losses have occurred frequently in animals, including lepidopteran insects. For example, the diurnal butterflies have more opsin genes than the nocturnal moths, which explains the spectral richness in butterfly eyes, at least in part (van der Kooi et al., 2021). However, the hawkmoths were found to switch their ecology from nocturnal to diurnal while keeping their opsin gene repertoire. To the best of my knowledge, the evolutionary process within a fixed set of opsins has never been properly addressed in the context of the diurnal–nocturnal transition. The present study on the hawkmoth opsins is unique in that it enables us to compare the opsin gene sequences and predicted opsin spectral sensitivities independently of the differences in gene number.

Why has gene duplication not occurred in hawkmoths? Gene duplication occurs mainly through recombination when two genes with similar sequences are located close to each other. In the *M. sexta* genome, the *LW* gene is located alone on chromosome 28. The *UV* and *SW* genes are located at a long distance apart on chromosome 15. The relationship between these two genes is widely conserved in other lepidopteran insects in which these genes are not duplicated (Gershman et al., 2021). Therefore, it is presumed that opsin gene duplication has been unlikely to occur in hawkmoths due to their genome structure, even though they have experienced light environment changes.

In addition to the opsin gene repertoire, I found no difference in the expression patterns of the three opsin genes between the diurnal and nocturnal hawkmoth species, while the evolutionary rates of amino acid substitutions differed significantly between them, although all ω values were below 1 (Table 3). Furthermore, many parallel amino acid substitutions between the different diurnal lineages

were observed in the three opsins (Figures 6 and 7, Table 4). These parallel substitutions exceeded the numbers expected under neutral evolution, suggesting that parallel evolution of the opsin sequences in diurnal species has probably been driven by positive selection. In the hawkmoths, the repertoire of opsin genes and the expression patterns of those genes have certainly been functionally constrained, preventing them from changing during the ecological transition from nocturnal to diurnal vision. Instead, the amino acid sequences of opsins would have been substituted by positive selection during the transitions, resulting in a large number of parallel amino acid substitutions. Although the effect of each parallel amino acid substitution on the function of the visual pigments is not known, the parallel substitutions possibly cause a functional change that is beneficial in the daylight environment.

Spectral shifts of visual pigments in diurnal–nocturnal transitions

I predicted the absorption spectra of the visual pigments based on the ERG-determined spectral sensitivities (Figure 8, Table 5). The λ_{max} values roughly match with those reported previously in the hawkmoths (van der Kooi et al., 2021). The determination of the visual pigments' absorption spectra is often tricky. Any of the currently available methods, such as ERG-recording, single-cell electrophysiology, microspectrophotometry, and *in vitro* expression, has its own strength and weakness. Here I employed the ERG-recording, which could have been accompanied by selective adaptation using monochromatic lights (Telles et al., 2014). However, I decided not to take this approach because even weak monochromatic lights can cause light adaptation of eyes presumably due to screening pigment migration which often makes the responses undetectable, particularly in the nocturnal species. Instead, I took the approach of increasing the number of samples (18–20 individuals for each species, Figure 8, Table 5), where I applied identical methods to all the individuals in both the nocturnal and diurnal species. The resulting spectral sensitivities were quite stable with small variations, and therefore the predicted visual pigment spectra were also steady. The results indicate that in two diurnal species, the peak absorption wavelength, λ_{max}, of *C. hylas* and *M. pyrrhosticta* shifts 16 nm and 5 nm in SW pigments towards long wavelength direction, and 15 nm and 6 nm in

LW pigments towards short wavelength direction, respectively.

Still, the model calculations deviate considerably, particularly in the UV region, and the contributions of SW pigments to the spectral sensitivities are estimated to be small (Figure 8). The difficult estimation is most likely due to the filtering effect of the screening pigments, which also exist in hawkmoth eyes (Figure 9). I could actually obtain better fits by incorporating presumptive pigment absorption spectra in the model. Even in the calculation with the function of the screening pigments, the predicted λ_{max} values are close to those without the pigments (Tables 5 and 6).

The shifts in the λ_{max} values are presumably attributed to the detected parallel amino acid substitutions. Figure 10 presents the common parallel substitutions in all the three diurnal lineages (D1–3): one for UV (I38V), and three for SW (I116V, V132I, T304A) and LW (I221V, M229L, F240Y) opsins. The probability of the parallel substitution occurring independently under neutral evolution in three lineages should be much smaller than in two lineages (Zhang and Kumar, 1997). There may be some synergistic effects of the amino acid substitutions, which would explain why some sites are far from the retinal chromophore (Figure 10). At any rate, these sites are the likely candidates for focusing future investigation of the molecular mechanism underlying the spectral shifts.

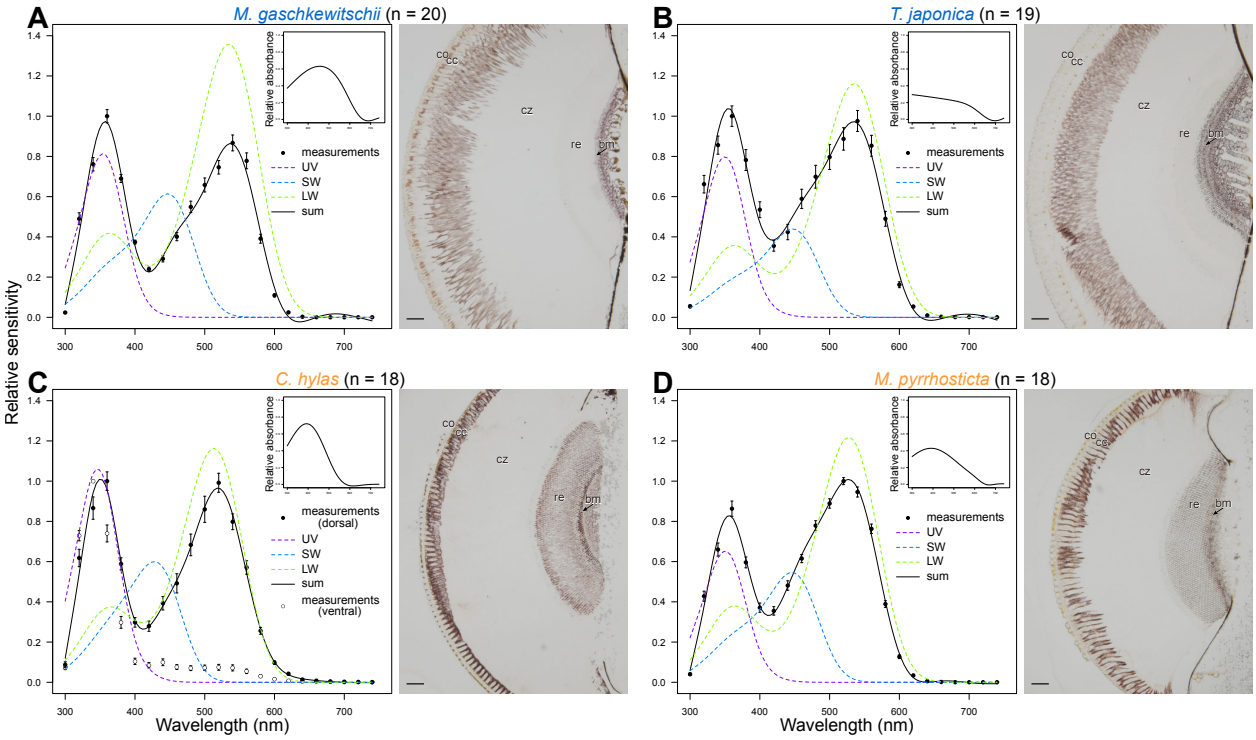

Figure 9. Spectral sensitivities of the compound eyes determined by ERG and the absorption spectra of visual pigments estimated with the effect of screening pigments. In the (A, B) nocturnal and (C, D) diurnal species, filled circles indicate mean ± SE of the measurements in multiple individuals, n, shown next to the species name. The open circles in panel C indicate the recorded sensitivity from the ventral eye region of *C. hylas* (n = 20: 16 males and 4 females). Dotted color lines are the absorption spectra of the individual visual pigments in the model fitting with the effect of the screening pigments. Solid line is the weighted sum of the three spectra minus the absorption spectrum of the screening pigments. Inset shows the spectrum of presumptive screening pigments. A frontal section of the compound eye is shown next to the spectral sensitivity. The clear zone (cz) separates the dioptric apparatus (crystalline cone, cc, and cornea, co) and the retina (re), where screening pigments reside. Arrow points to the position of the basement membrane (bm). Scale bar = 100 μm.

The model fitting to the ERG data indicated that the contribution of UV and SW pigments were equally high, while LW pigments contributed most (Tables 5 and 6). The results fitted even better to the results of the expression ratios of the opsin genes (Figure 3). The estimated λ_{max} values of UV and LW pigments were also similar: importantly, the shift direction and the amount both in LW pigments appear robust (Tables 5 and 6). On the other hand, for the estimated λ_{max} values of SW pigments the

shift direction was opposite (Tables 5 and 6). This contradictory result is probably led by an inaccurate estimation due to the overlap of the absorption peak of SW pigments and the Gaussian mound in the screening pigments' absorption spectrum. Thus, measurement of the absorbance spectra of the screening pigments in the hawkmoths is warranted in the future.

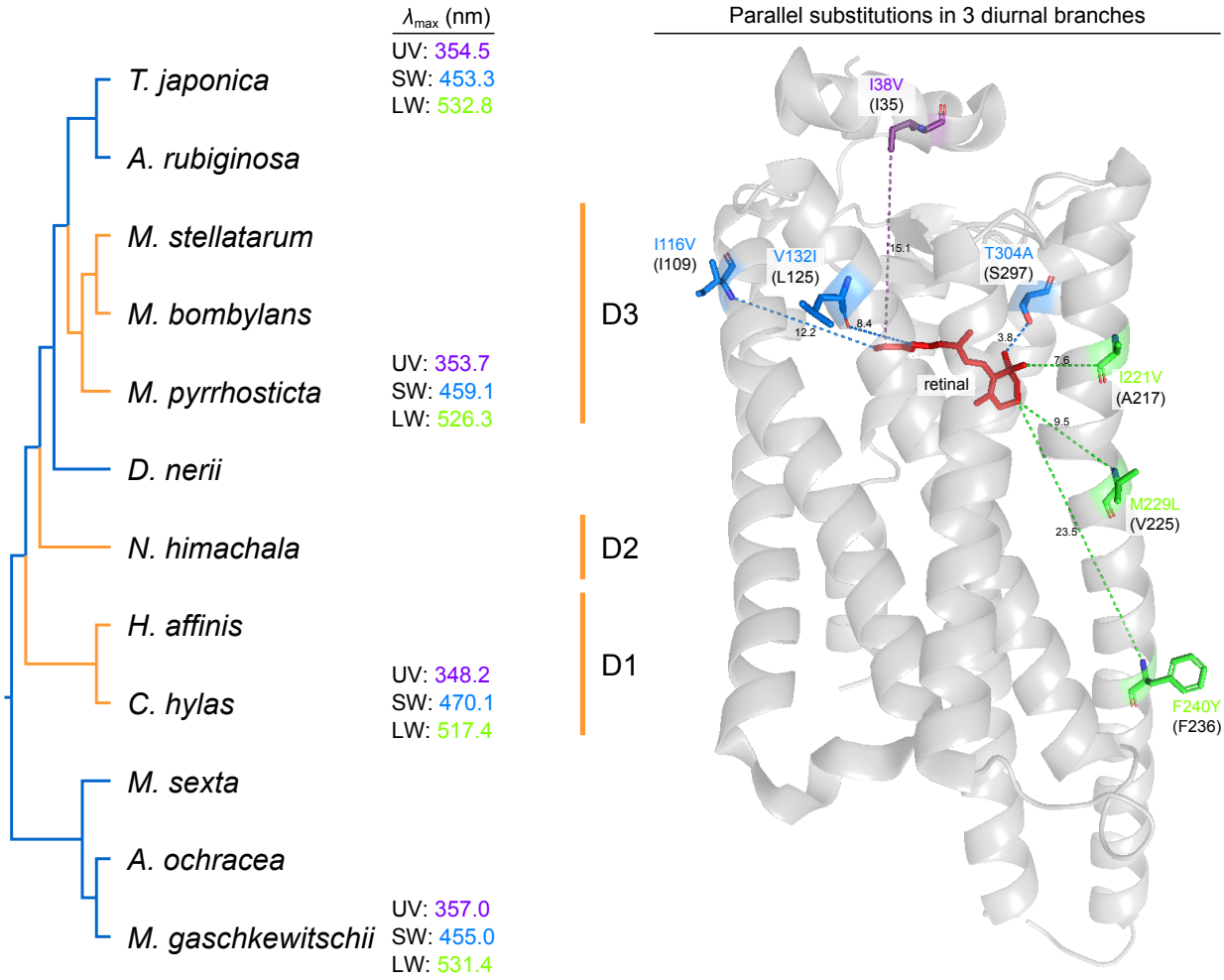

Figure 10. Common parallel substitutions among the three diurnal branches and absorption spectra of the opsin visual pigments. The tree topology is based on the phylogenetic tree of hawkmoth species (Figure 2). The indigo and orange branches are nocturnal and diurnal, respectively. The λ_{max} values of the three visual pigments estimated in this study are shown on the right side of the species names. For the three opsins, the common parallel amino acid substitutions occurring in the three diurnal branches are shown on the right side of the diurnal clade names D1–3, and those positions are indicated on the 3D model of jumping spider Rh1 opsin. The minimum distances (Å) between the retinal chromophore (red) and the amino acid positions are depicted by dotted color lines. Corresponding amino acid positions in jumping spider Rh1 are shown in the parentheses under the amino acid substitutions. The colors of the λ_{max} values and the substitutions represent the three opsin pigments: violet, UV pigment; blue, SW pigment; green, LW pigment. Amino acid residue numbers for the substitutions follow those of each orthologous opsin in *M. sexta*.

Table 6. Parameters of the absorption spectra of visual and screening pigments in the hawkmoth species

		Visual pigments									Screening pigment					
Model	Species	UV λ_{max} (nm)	Mean ($\Delta\lambda_{max}$ from Noct.) (nm)	SW λ_{max} (nm)	Mean ($\Delta\lambda_{max}$ from Noct.) (nm)	LW λ_{max} (nm)	Mean ($\Delta\lambda_{max}$ from Noct.) (nm)	UV amplitude f_{UV} (relative ratio, %)	SW amplitude f_{SW} (relative ratio, %)	LW amplitude f_{LW} (relative ratio, %)	μ_1 (nm)	σ_1 (nm)	p_1	μ_2 (nm)	σ_2 (nm)	p_2
$S_e(\lambda) = S(\lambda) - A(\lambda)$	*M. gaschkewitschi* (n = 20)	353.1	350.6	448.3	448.4	534.4	534.9	0.633 (24.4%)	0.606 (23.3%)	1.358 (52.3%)	459.8	154.5	0.634	652.3	63.9	-0.269
	T. japonica (n = 19)	348.1		448.4		535.4		0.626 (28.2%)	0.434 (19.5%)	1.162 (52.3%)	0.0095	543.2	0.344	689.1	63.8	-0.168
	C. hylas (n = 18)	344.5	346.7 (-3.9)	431.3	439.4 (-9.0)	513.0	520.3 (-14.6)	0.837 (32.5%)	0.575 (22.3%)	1.163 (45.2%)	408.8	107.2	0.771	533.1	73.1	-0.262
	M. pyrrhosticta (n = 18)	348.8		447.5		527.5		0.511 (22.5%)	0.539 (23.8%)	1.218 (53.7%)	390.7	125.9	0.429	653.0	34.6	-0.048

Relationship between hawkmoth vision and light environments

The visual pigments mainly function in the eyes. An insect's compound eye consists of thousands of small units called ommatidia, each typically containing eight or nine photoreceptor cells. The photoreceptor cells together form a visual pigment-containing rhabdom. The visual pigments absorb the light propagating in the rhabdom and trigger the phototransduction cascade, which eventually depolarizes the photoreceptor membrane. Although examples of co-expression of opsin genes have been reported in insects (Arikawa and Stavenga, 2014), one photoreceptor is typically assumed to express one type of opsin corresponding to a particular visual pigment, whose absorption spectrum principally determines the photoreceptor's spectral sensitivity. Accumulated evidence indicates that an ommatidium generally bears seven LW opsin-expressing photoreceptor cells and two UV or SW opsin-expressing cells (van der Kooi et al., 2021). Hence, the ratio roughly matches the opsin gene expression ratio I found in the hawkmoths (Figure 3), implying that the predominant expression of the *LW* gene has been evolutionarily conserved by constraints on the distribution of the photoreceptor cells in the rhabdom. Note also that the combination of UV or SW opsin-expressing cells is three ways: two UVs, two SWs, or one each, making the ommatidia spectrally heterogeneous. These three types of ommatidia randomly fill the hexagonal lattice at least locally (Arikawa and Stavenga, 2014). The basic spectral organization of ommatidia and their random array also hold for the Tobacco hawkmoth, *M. sexta* (White et al., 2003).

The LW opsin-expressing photoreceptors are green-sensitive in most cases. However, some of the LW opsin-expressing cells are red-sensitive in the ommatidia of pierid butterflies, where the dense reddish pigments surround the rhabdom (Stavenga and Arikawa, 2011). The perirhabdomal pigments alter the spectral contents of the light propagating in the thin rhabdom by absorbing the boundary wave, thus changing the cell's spectral sensitivity. In the hawkmoth eyes, I did not find any sign of such perirhabdomal pigments (Figure 9). Plus, the diameter of the hawkmoths' rhabdom is large (Warrant et al., 1999), which prevents the perirhabdomal pigments, if any, from functioning as a robust spectral filter. Therefore, the absence of perirhabdomal pigments suggests that LW opsin-expressing

cells in hawkmoth eyes are most likely to be green-sensitive.

The green receptors exceed in number, and they localize in all ommatidia making a complete hexagonal lattice in the compound eye. In contrast, the distribution of UV and blue receptors has gaps because of the random array. The complete hexagonal lattice of the green receptor system is presumably crucial in achromatic spatial and motion vision (Yamaguchi et al., 2008; Stewart et al., 2015). The green receptors also contribute to color vision (von Helversen, 1972; Koshitaka et al., 2008), and UV-blue-green trichromacy has been proposed in the Hummingbird hawkmoth, *M. stellatarum* (Telles et al., 2016).

Parallel evolution in diurnal hawkmoth opsin sequences may have been caused by positive selection pressures most likely to be adaptive for daytime activity. Compared with the nocturnal *D. elpenor*, the diurnal *M. stellatarum* puts more weight on visual cues than olfactory ones (Balkenius et al., 2006; Stöckl et al., 2016). As described above, the λ_{max} values of LW and SW pigments in the diurnal species shifted 10 nm in short and long wavelength direction, respectively: the separation of the sensitivity spectra of these cells has become 20 nm smaller. For color vision, a 20 nm difference in the photoreceptor $S(\lambda)$ is not negligible: human color deficiency can be attributed to only several nanometer differences in the cone $S(\lambda)$ (Bowmaker, 1998), and *M. stellatarum* with trichromatic vision discriminates the wavelength differences of 1–2 nm at around 380 nm and 480 nm, which correspond to the wavelength regions where the spectral sensitivities of the photoreceptors overlap (Telles et al., 2016). The *Papilio* butterfly with tetrachromatic vision also discriminates the wavelength differences of a few nanometres (Koshitaka et al., 2008). The large separation between λ_{max} values of the visual pigments in the nocturnal species widens the visible spectral range, which could gain absolute sensitivity in a light-limited environment (Johnsen et al., 2006). On the other hand, the reduced λ_{max} separation increases the overlap of the spectral sensitivities, which potentially enhances the wavelength discrimination that the diurnal species can utilize. The reduced λ_{max} separation has also been recently reported in the *Heliconius* butterflies which have lost the UV2 receptor (McCulloch et al., 2022). Specially in *Heliconius ismenius*, the λ_{max} values of the UV1 and

blue receptors are shifted toward longer and shorter wavelengths, respectively. This reduced λ_{max} separation in *H. ismenius* may enhance color discrimination in the short wavelength range owing to a greater overlap of the spectral sensitivities between the UV1 and blue receptors compared with that of *Heliconius melpomene*. In two diurnal hawkmoths, the separation between λ_{max} values of the visual pigments were different: 47 nm in *C. hylas* and 67 nm in *M. pyrrhosticta*. The difference in these values may be related to differences in wavelength discrimination ability, i.e., *C. hylas* has higher discrimination ability than that of *M. pyrrhosticta*.

Because I focused on determining the absorption spectra of the visual pigments, I did not extend the analysis to dorso-ventral specialization. Nevertheless, I have indeed noticed that the ventral eye region of *C. hylas* was almost exclusively sensitive to UV (Figure 9C), which seems unique to this species. Inverted cases are known in other insects, including *M. sexta* where more UV opsin-expressing photoreceptors are distributed in the dorsal region of the eye (White et al., 2003), which is consistent with the dorsal region being more sensitive to UV (Bennett et al., 1997). In the diurnal owl-fly, *Libelloides macaronius*, for instance, the dorsal region exclusively sensitive to UV is optimal for owl-flies detecting small flying targets against the bright sky (Belušič et al., 2013). More detailed analyses of the anatomical distribution of visual pigments, the physiological properties of eyes and associated visual behavior will further shed light on adaptive evolution of hawkmoth opsins through their diurnal–nocturnal transition.

Chapter 6. Conclusions and General Discussion

In the current study of nocturnal and diurnal hawkmoths, I identified the opsin genes, their expression levels, and possible absorption spectra of visual pigments. The transitions from nocturnal to diurnal ecologies in the closely related hawkmoth species were accompanied by parallel amino acid substitutions in visual opsins, which presumably brought spectral sensitivities of LW and SW pigments closer and enhanced their color discrimination properties.

I will attempt to connect my findings on parallel evolution of vision among hawkmoth species through the diurnal–nocturnal transition to history of evolutionary biology in several different ways, to provide some fragmentary hints to the knowledge, below.

Parallel evolution at amino acid sequence level

I have detected different amino acid substitution rates comparing nocturnal with diurnal in all the three opsin sequences, and discovered the unusually excessive numbers of the parallel substitutions between the diurnal opsins: maximum 14 sites in LW opsins (Figure 6, Table 4). Then, the gene tree topology of the UV opsin tree reflects the species' phylogenetic relationships, in contrast the topologies of SW and LW opsins reflect the nocturnal and diurnal ecology (Figure 5). It has been suggested that parallel events at the amino acid level occur very rarely, and hardly ever affect the gene tree topology in the comparison of similar sequences where closely related species or a large number of operational taxonomic units (OTUs) are treated (Doolittle, 1994; Kreitman and Akashi, 1995; Adachi and Hasegawa, 1996). However, the present study of the opsin genes in hawkmoth species has uniquely demonstrated the interesting case evidence in which strong parallel evolution has the drastic effect on the topology of the reconstructed gene tree based on the amino acid sequences in closely related species by the ML method after the classic studies on parallel evolution of the stomach lysozymes in foregut fermenters (Stewart et al., 1987; Swanson et al., 1991; Zhang and Kumar, 1997; Nei and Kumar, 2000).

I showed the numbers of parallel substitutions cannot be explained by evolutionary contingency, and consequently the substitutions may have been necessarily caused by parallel evolution under positive natural selection on SW and LW opsins of all the diurnal species, and on UV opsins of the diurnal *C. hylas*, *H. affinis* and *Macroglossum* species. The statistical results of the *N. himachala–M. pyrrhosticta* and the *N. himachala–M. bombylans* pairs in UV opsins were positive, whereas the *N. himachala–M. stellatarum* pair which had only the same I38V substitution tested negative (Table 4). This incompatible result is likely due to the reason that a parallel deletion (ΔP372) on the lineage pairs in UV opsins was not included in the current statistical test for parallel evolution, other than to the conditions of the background sequences.

Besides the spectral sensitivities of the compound eyes, the localization of the screening pigments in the retina (Figure 9) and other visual phenotypes (e.g., the numbers of the facets, the morphologies of the lamina monopolar cells [LMCs] in the optic lobe, and the responses of the motion-sensitive neurons in the lobula complex) (Stöckl et al., 2017) also differ between the nocturnal and diurnal hawkmoth species. Therefore, to evaluate the particularity/universality of the parallel evolutionary pattern found in the opsin genes and the impact range of the diel niches on genes, it would be worthwhile to investigate if other light-interacting genes have also caused such evolutionary pattern in the nocturnal and diurnal hawkmoths.

Relationship between evolutionary changes in gene expression level and in amino acid sequence level

I showed the RNA-seq analysis shows that *LW* gene presents the highest mRNA expression ratio among three opsin genes in the eyes of all hawkmoths, and the transcript pattern is not affected by the difference of diel periodicities (Figures 3 and 4). I also estimated the relative contribution of the three visual pigments to the ERG-determined spectral sensitivities of the eyes, and showed that LW pigment possesses the highest amplitude in all species (Figures 8 and 9, Tables 5 and 6). This latter result from the spectral sensitivity corresponds with the former result of the opsin gene expression level.

So, I discuss that one of the probable reasons for which LW opsin is predominantly held can be considered to lie in the distribution of the photoreceptor cells, i.e., it is the common arrangement widely across the insects that the photoreceptors containing LW pigment are most often localized in the rhabdom in the compound eyes (Briscoe, 2008; Wakakuwa et al., 2010; Friedrich et al., 2011; Matsushita et al., 2012; van der Kooi et al., 2021). The expression comparison of opsin genes between a nocturnal moth, *M. sexta*, and a diurnal butterfly, *H. melpomene*, shows higher expression levels of the three visual opsin genes in the diurnal butterfly (Macias-Muñoz et. al., 2019). The opsin gene expressions in some African cichlid fishes differ among the species, and then the difference tunes their spectral sensitivities (Carleton and Kocher, 2001). It has been suggested that phenotypic differences are frequently due to differences in the regulations of gene expressions rather than to differences in the amino acid sequences of proteins (Zuckerkandl and Pauling, 1965; King and Wilson, 1975). I found that the evolutionary rates of amino acid substitutions were significantly different between the nocturnal and diurnal hawkmoth opsins. However, although the mRNA expressions of opsin genes in *H. armigera* exhibit the circadian rhythms (Yan et al., 2014) and my transcript data were collected at the same hour in the day from all the hawkmoths (Table 1), both nocturnal and diurnal species showed the same gene expression pattern. I thus conjecture that the expression pattern of the opsin genes has been evolutionarily conservative due to the constraints related to the insect visual systems strong enough to outweigh the influence of the switch of diurnal–nocturnal activities in the closely related hawkmoth species.

Spectral tuning sites of opsin visual pigments in lepidopteran insects

Combining the physiological difference of the spectral sensitivities together with the results of the molecular evolutionary analyses of the opsins, the results suggest that parallel evolution of the opsins probably driven by positive Darwinian selection likely have caused adaptive phenotypic convergence of the spectral sensitivity functions of vision among the closely related diurnal hawkmoths. Still, it is unclear which mutations in the opsin proteins are critical for the absorption shift and/or how they are

involved in the functional change. As the most likely candidate amino acid sites for the spectral shifts, there are the common parallel substitutions among the three diurnal branches in all the clades D1–3 for all the three opsins (Figure 10), which are far less probable to occur than parallel evolution on two branches (Zhang and Kumar, 1997). It is notably noteworthy that all the three sites of LW opsin are located together in TM helix 5 (Figure 10).

Furthermore, some parallel sites in the present study correspond with the spectral tuning sites in the invertebrate opsins predicted by the previous studies which inquire with electrophysiological experiments: S230T in UV opsin; A235T in SW opsin; S70C, A140G, F189M, I221V, M229L and L232F in LW opsin (Briscoe, 2001, 2002; Frentiu et al., 2007; Briscoe et al., 2010; Chung and Marshall, 2016) (Figures 7 and 10). On the other hand, the evidence that the huge numbers of the parallel changes have occurred in the diurnal hawkmoth opsins implies that their compositive effects through synergistic interactions possibly achieve the functional changes of the visual pigments: for example, the structural distortion of the opsin protein which changes absorption spectra may be caused by the combination of multiple substitutions, or internal substitutions close to the retinal chromophore may be essential for the spectral shifts and external ones may contribute to the protein stability (Baldwin et al., 1996; Yokoyama, 2008). This can be a possible reason there are the amino acid substitutions at positions both near and far from the retinal in the opsins (Figures 7 and 10). Besides, some mutations might potentially involve functions other than the wavelength shifting, e.g., the rhodopsin synthesis and transport (Bentrop et al., 1997), or the protein fold (Mackin et al., 2014).

The invertebrate G_q-coupled opsin is variously different from the vertebrate G_t-coupled opsin in terms of the metarhodopsin state, the phototransduction cascades, etc. (Hamdorf, 1979; Stavenga, 1995; Hardie and Postma, 2008; Yau and Hardie, 2009; Hardie and Franze, 2012), and the effect of the spectral tuning sites is dependent on interactions with the amino acid residues at other sites of the opsin (Yokoyama, 2008; Dungan and Chang, 2017). Therefore, it is questionable if the spectral tuning sites in the vertebrate opsins can be applied to the invertebrates, but the clear tuning sites in the lepidopteran insects showed by *in vitro* reconstitution of the visual pigments and site-directed

mutagenesis have rarely been reported, until recently (Wakakuwa et al., 2010; Saito et al., 2019; Liénard et al., 2021). Recently the methods, i.e., heterologous action spectroscopy and parallel sensitive heterologous expression, have been developed (Sugihara et al., 2016; Saito et al., 2019; Liénard et al., 2021; 2022), thus it is expected to find out in the future which substitutions found in the present study are important for the functional evolution and how they cause the physiological change.

Phylogenetic divergences of diurnal hawkmoths

I showed the phenotypic homoplasy by parallelism for the diurnal/nocturnal activity across closely related species belonging to one family using the species tree from the multilocus data. Becoming diurnal has occurred independently at least three times in the subfamily Macroglossinae in the relatively short time scale after hawkmoth divergence. Huang et al. (2022) estimates the divergence times of the diurnal hawkmoths by using mitochondrial DNA (mtDNA). In the estimate, *Neogurelca himachala* (D2 in Figure 2) appeared around 29.2 MYA, subtribe Hemarina (genus *Cephonodes* and *Hemaris*) lineage (D1) appeared around 25.8 MYA, and genus *Macroglossum* lineage (D3) appeared 19.3 MYA (Huang et al., 2022). Both the phylogenetic tree based on transcriptome sequence in this study and the phylogenetic tree based on mtDNA in Huang et al. (2022) indicate the relatively recent and independent appearances of the diurnal lineages, but the phylogenetic relationships are partially conflicting. Therefore, genome-wide sequence data from more dense taxon sampling are needed to untangle the evolutionary history of nocturnal and diurnal hawkmoths.

Adaptive evolution of hawkmoth vision

Nocturnal to diurnal transitions in hawkmoths are accompanied by reduced separation between short- and long-wavelength sensitivity peaks which may be caused by rapid parallel amino acid substitutions in visual opsins. The diurnal hawkmoths may have enhanced color discrimination ability in the blue-green range under daylight. Why is the evolution of the hawkmoths' visual system so

strongly linked to the day and night light environments compared to other terrestrial animals such as primates or butterflies, which have also become diurnal? I discuss how opsin gene duplication in hawkmoths in the first place has been unlikely to occur due to their genome structure. To show adaptive evolution, I should show all of the following criteria: an amino acid change, a functional change of a protein caused by the amino acid change, and an increase of fitness by the functional change of the protein. But, if I am allowed to give a little of my speculation, it may be responsible for the link between the hawkmoth vision and light environments that both (1) the closely related diurnal hawkmoths have only diverged for a short evolutionary time period, and probably in relation to the time scale, (2) their visual behavior and communication, such as the use of signals by color vision, have not yet evolved to be as important and various as in other diurnal animals. Therefore, I hypothesize the effect of a drastic change from night to day light environments simply appeared as selective pressure strong enough for directional selection to act on the visual system of diurnal hawkmoths. I believe that, to my knowledge, it is one of the best cases showing the strength of light environmental effects on evolution of vision, which has not been found in any other terrestrial animals before.

Acknowledgements

I would like to thank the principal advisor Professor Dr. Kentaro Arikawa, PhD, (SOKENDAI) for the guidance and criticism on my PhD research. I am very glad for the advice on physiological and histological experiments. I would like to thank the co-advisor Assistant Professor Dr. Yohey Terai, PhD, (SOKENDAI) for the advice on molecular biological experiments and molecular evolutionary analyses. I also thank another co-advisor Associate Professor Dr. Michiyo Kinoshita, PhD, (SOKENDAI) for the tutelage of basic experiments with insects.

I wish to thank Professor Dr. Shunsuke Yajima, PhD, and Dr. Hironobu Uchiyama (Tokyo University of Agriculture) for next generation sequencing (NGS).

I wish to thank Assistant Professor Dr. Finlay J. Stewart, PhD, for the technical advice on model fitting to ERG data, Assistant Professor Dr. Hisao Tsukamoto, PhD, for the suggestion on interpretation of the amino acid substitutions in opsin, Dr. Motohiro Wakakuwa for the technical advice on molecular biological experiments, Drs. Primož Pirih and Hisaharu Koshitaka for the technical advice on electrophysiology, Dr. Hiroshi D. Akashi for the suggestion on RNA-seq analyses, and Dr. Takashi Seiko and Ken Nagata (SOKENDAI) for the suggestion on molecular evolutionary analyses. I also thank the members of SOKENDAI on the Hayama campus for fruitful discussions and comments.

I am particularly grateful to Izumi Akiyama (Jiyu Gakuen) and Mizuha Akiyama (Keio University) for help with collecting hawkmoth samples. I am grateful to Professor Yoshimi Akiyama (Chuo University) for English editing.

I sincere thank the Cooperative Research Grant of the Genome Research for BioResource, NODAI Genome Research Center, Tokyo University of Agriculture for the financial support to RNA sequencing.

Lastly, it is a pleasure to express special thanks to all of my dear friends and my family who have ceaselessly encouraged and supported my research life.

References

Abouheif, E. (2008). Parallelism as the pattern and process of mesoevolution. *Evol. Dev.* **10**, 3-5.

Adachi, J. and Hasegawa, M. (1996). *MOLPHY Version 2.3: Programs for Molecular Phylogenetics Based on Maximum Likelihood*. Tokyo, Japan: Institute of Statistical Mathematics.

Altschul, S. F., Gish, W., Miller, W., Myers, E. W. and Lipman, D. J. (1990). Basic local alignment search tool. *J. Mol. Biol.* **215**, 403-410.

Arikawa, K., Mizuno, S., Scholten, D. G. W., Kinoshita, M., Seki, T., Kitamoto, J. and Stavenga, D. G. (1999). An ultraviolet absorbing pigment causes a narrow-band violet receptor and a single-peaked green receptor in the eye of the butterfly *Papilio*. *Vision Res.* **39**, 1-8.

Arikawa, K. and Stavenga, D. G. (2014). Insect photopigments: Photoreceptor spectral sensitivities and visual adaptations. In *Evolution of Visual and Non-visual Pigments* (eds. D. M. Hunt, M. W. Hankins, S. P. Collin and N. J. Marshall). In *Springer Series in Vision Research* (eds. N. J. Marshall and S. P. Collin), vol. 4, pp. 137-162. Boston, MA, USA: Springer.

Baldwin, E., Xu, J., Hajiseyedjavadi, O., Baase, W. A. and Matthews, B. W. (1996). Thermodynamic and structural compensation in "size-switch" core repacking variants of bacteriophage T4 lysozyme. *J. Mol. Biol.* **259**, 542-559.

Balkenius, A., Rosén, W. and Kelber, A. (2006). The relative importance of olfaction and vision in a diurnal and a nocturnal hawkmoth. *J. Comp. Physiol. A.* **192**, 431-437.

Belušič, G., Pirih, P. and Stavenga, D. G. (2013). A cute and highly contrast-sensitive superposition eye – the diurnal owlfly *Libelloides macaronius*. *J. Exp. Biol.* **216**, 2081-2088.

Bennett, R. R., White, R. H. and Meadows, J. (1997). Regional specialization in the eye of the sphingid moth *Manduca sexta*: Blue sensitivity of the ventral retina. *Vis. Neurosci.* **14**, 523-526.

Bentrop, J., Schwab, K., Pak, W. L. and Paulsen, R. (1997). Site-directed mutagenesis of highly conserved amino acids in the first cytoplasmic loop of *Drosophila* Rh1 opsin blocks rhodopsin synthesis in the nascent state. *EMBO J.* **16**, 1600-1609.

Bowmaker, J. K. (1998). Visual pigments and molecular genetics of color blindness. *News Physiol. Sci.* **13**, 63-69.

Briscoe, A. D. (2001). Functional diversification of lepidopteran opsins following gene duplication. *Mol. Biol. Evol.* **18**, 2270-2279.

Briscoe, A. D. (2002). Homology modeling suggests a functional role for parallel amino acid substitutions between bee and butterfly red- and green-sensitive opsins. *Mol. Biol. Evol.* **19**, 983-986.

Briscoe, A. D. (2008). Reconstructing the ancestral butterfly eye: focus on the opsins. *J. Exp. Biol.* **211**, 1805-1813.

Briscoe, A. D., Bybee, S. M., Bernard, G. D., Yuan, F., Sison-Mangus, M. P., Reed, R. D., Warren, A. D., Llorente-Bousquets, J. and Chiao, C.-C. (2010). Positive selection of a duplicated UV-sensitive visual pigment coincides with wing pigment evolution in *Heliconius* butterflies. *Proc. Natl. Acad. Sci. U S A.* **107**, 3628-3633.

Cao, Y., Adachi, J., Janke, A., Pääbo, S. and Hasegawa, M. (1994). Phylogenetic relationships among eutherian orders estimated from inferred sequences of mitochondrial proteins: Instability of a tree based on a single gene. *J. Mol. Evol.* **39**, 519-527.

Carleton, K. L. and Kocher, T. D. (2001). Cone opsin genes of African cichlid fishes: tuning spectral sensitivity by differential gene expression. *Mol. Biol. Evol.* **18**, 1540-1550.

Chase, M. R., Bennett, R. R. and White, R. H. (1997). Three opsin-encoding cDNAS from the compound eye of *Manduca sexta*. *J. Exp. Biol.* **200**, 2469-2478.

Chen, L., Wang, X.-Y., Lu, W. and Zheng, X.-L. (2021). Sexual communication in diurnal moths: behaviors and mechanisms. *Int. J. Trop. Insect Sci.* **41**, 15-24.

Chung, W.-S. and Marshall, N. J. (2016). Comparative visual ecology of cephalopods from different habitats. *Proc. Biol. Sci.* **283**, 20161346.

Cronin, T. W., Johnsen, S., Marshall, N. J. and Warrant, E. J. (2014). *Visual Ecology*. Princeton, NJ, USA: Princeton University Press.

Darwin, C. (1859). *On the Origin of Species by Means of Natural Selection, or the Preservation of Favoured Races in the Struggle for Life*. London, UK: J. Murray.

Dobzhansky, T. (1954). Evolution as a creative process. *Proc. 9th Int. Congr. Genet., Caryologia* **6** (Suppl.), 435-449.

Doolittle, R. F. (1994). Convergent evolution: the need to be explicit. *Trends Biochem. Sci.* **19**, 15-18.

Dungan, S. Z. and Chang, B. S. W. (2017). Epistatic interactions influence terrestrial–marine functional shifts in cetacean rhodopsin. *Proc. Biol. Sci.* **284**, 20162743.

Elzhov, T. V., Mullen, K. M., Spiess, A.-N. and Bolker, B. (2016). *minpack.lm: R Interface to the Levenberg-Marquardt Nonlinear Least-Squares Algorithm Found in MINPACK, Plus Support for Bounds*: CRAN. https://CRAN.R-project.org/package=minpack.lm.

Esaki, T., Issiki, S., Mutuura, A., Inoue, H., Okagaki, H., Ogata, M. and Kuroko, H. (1971). *Icones Heterocerorum Japonicorum in Coloribus Naturalibus (Moths of Japan in Color Vol. II)*. Higashiosaka, Japan: Hoikusha Publishing Co., Ltd. (in Japanese).

Felsenstein, J. (1985). Confidence limits on phylogenies: an approach using the bootstrap. *Evolution* **39**, 783-791.

Feuda, R., Marlétaz, F., Bentley, M. A. and Holland, P. W. H. (2016). Conservation, duplication, and divergence of five opsin genes in insect evolution. *Genome Biol. Evol.* **8**, 579-587.

Frentiu, F. D., Bernard, G. D., Sison-Mangus, M. P., Brower, A. V. Z. and Briscoe, A. D. (2007). Gene duplication is an evolutionary mechanism for expanding spectral diversity in the long-wavelength photopigments of butterflies. *Mol. Biol. Evol.* **24**, 2016-2028.

Friedrich, M., Wood, E. J. and Wu, M. (2011). Developmental evolution of the insect retina: insights from standardized numbering of homologous photoreceptors. *J. Exp. Zool. B Mol. Dev. Evol.* **316**, 484-499.

Gerkema, M. P., Davies, W. I. L., Foster, R. G., Menaker, M. and Hut, R. A. (2013). The nocturnal bottleneck and the evolution of activity patterns in mammals. *Proc. Biol. Sci.* **280**, 20130508.

Gershman, A., Romer, T. G., Fan, Y., Razaghi, R., Smith, W. A. and Timp, W. (2021). *De novo* genome assembly of the tobacco hornworm moth (*Manduca sexta*). *G3 (Bethesda)* **11**, jkaa047.

Goyret, J., Pfaff, M., Raguso, R. A. and Kelber, A. (2008). Why do *Manduca sexta* feed from white flowers? Innate and learnt colour preferences in a hawkmoth. *Naturwissenschaften* **95**, 569-576.

Hamdorf, K. (1979). The physiology of invertebrate visual pigments. In *Comparative Physiology and Evolution of Vision in Invertebrates. Handbook of Sensory Physiology, vol 7 / 6 / 6 A* (ed. H. Autrum), pp. 145-224. Berlin and Heidelberg, Germany: Springer.

Hardie, R. C. and Franze, K. (2012). Photomechanical responses in *Drosophila* photoreceptors. *Science* **338**, 260-263.

Hardie, R. C. and Postma, M. (2008). Phototransduction in microvillar photoreceptors of *Drosophila* and other invertebrates. In *The Senses: A Comprehensive Reference* (eds. A. I. Basbaum, A. Kaneko, G. M. Shepherd and G. Westheimer)*, Vol. 1: Vision I* (eds. R. H. Masland and T. D. Albright), pp. 77-130. San Diego, CA, USA: Academic Press.

Hothorn, T. and Hornik, K. (2019). *exactRankTests: Exact Distributions for Rank and Permutation Tests*: CRAN. https://CRAN.R-project.org/package=exactRankTests.

Huang, Y.-X., Xing, Z.-P., Zhang, H., Xu, Z.-B., Tao, L.-L., Hu, H.-Y., Kitching, I. J. and Wang, X. (2022). Characterization of the complete mitochondrial genome of eight diurnal hawkmoths (Lepidoptera: Sphingidae): new insights into the origin and evolution of diurnalism in sphingids. *Insects* **13**, 887.

Johnsen, S., Kelber, A., Warrant, E., Sweeney, A. M., Widder, E. A., Lee, R. L. and Hernández-Andrés, J. (2006). Crepuscular and nocturnal illumination and its effects on color perception by the nocturnal hawkmoth *Deilephila elpenor*. *J. Exp. Biol.* **209**, 789-800.

Jones, D. T., Taylor, W. R. and Thornton, J. M. (1992). The rapid generation of mutation data matrices from protein sequences. *Comput. Appl. Biosci.* **8**, 275-282.

Kanost, M. R. Arrese, E. L. Cao, X. Chen, Y.-R. Chellapilla, S. Goldsmith, M. R. Grosse-Wilde, E. Heckel, D. G. Herndon, N. Jiang, H. et al. (2016). Multifaceted biological insights from a

draft genome sequence of the tobacco hornworm moth, *Manduca sexta*. *Insect Biochem. Mol. Biol.* **76**, 118-147.

Kawahara, A. Y., Mignault, A. A., Regier, J. C., Kitching, I. J. and Mitter, C. (2009). Phylogeny and biogeography of hawkmoths (Lepidoptera: Sphingidae): evidence from five nuclear genes. *PLoS One* **4**, e5719.

Kawahara, A. Y., Plotkin, D., Espeland, M., Meusemann, K., Toussaint, E. F. A., Donath, A., Gimnich, F., Frandsen, P. B., Zwick, A., dos Reis, M. et al. (2019). Phylogenomics reveals the evolutionary timing and pattern of butterflies and moths. *Proc. Natl. Acad. Sci. USA* **116**, 22657-22663.

Kawahara, A. Y., Plotkin, D., Hamilton, C. A., Gough, H., St Laurent, R., Owens, H. L., Homziak, N. T. and Barber, J. R. (2018). Diel behavior in moths and butterflies: a synthesis of data illuminates the evolution of temporal activity. *Org. Divers. Evol.* **18**, 13-27.

Kawamura, S. (2011). Evolutionary diversification of visual opsin genes in fish and primates. In *From Genes to Animal Behavior: Social Structures, Personalities, Communication by Color* (eds. M. Inoue-Murayama, S. Kawamura and A. Weiss). In *Primatology Monographs* (eds. T. Matsuzawa and J. Yamagiwa), pp. 329-349. Tokyo, Japan: Springer.

Kawamura, S. (2016). Color vision diversity and significance in primates inferred from genetic and field studies. *Genes Genomics* **38**, 779-791.

Kelber, A. (1997). Innate preferences for flower features in the hawkmoth *Macroglossum stellatarum*. *J. Exp. Biol.* **200**, 827-836.

Kelber, A., Balkenius, A. and Warrant, E. J. (2002). Scotopic colour vision in nocturnal hawkmoths. *Nature* **419**, 922-925.

Kimura, M. (1968). Evolutionary rate at the molecular level. *Nature* **217**, 624-626.

King, J. L. and Jukes, T. H. (1969). Non-Darwinian evolution. *Science* **164**, 788-798.

King, M.-C. and Wilson, A. C. (1975). Evolution at two levels in humans and chimpanzees. *Science* **188**, 107-116.

Kishida, Y. (2011). *The Standard of Moths in Japan 1*. Tokyo, Japan: Gakken Education Publishing. (in Japanese).

Kishino, H., Miyata, T. and Hasegawa, M. (1990). Maximum likelihood inference of protein phylogeny and the origin of chloroplasts. *J. Mol. Evol.* **31**, 151-160.

Kitching, I. J. and Cadiou, J.-M. (2000). *Hawkmoths of the World: an Annotated and Illustrated Revisionary Checklist (Lepidoptera: Sphingidae)*. Ithaca, NY, USA: Cornell University Press.

Koshitaka, H., Kinoshita, M., Vorobyev, M. and Arikawa, K. (2008). Tetrachromacy in a butterfly that has eight varieties of spectral receptors. *Proc. Biol. Sci.* **275**, 947-954.

Kreitman, M. and Akashi, H. (1995). Molecular evidence for natural selection. *Annu. Rev. Ecol. Syst.* **26**, 403-422.

Krogh, A., Larsson, B., von Heijne, G. and Sonnhammer, E. L. L. (2001). Predicting transmembrane protein topology with a hidden markov model: application to complete genomes. *J. Mol. Biol.* **305**, 567-580.

Kumar, S., Stecher, G. and Tamura, K. (2016). MEGA7: Molecular Evolutionary Genetics Analysis version 7.0 for bigger datasets. *Mol. Biol. Evol.* **33**, 1870-1874.

Land, M. F. and Nilsson, D.-E. (2012). *Animal Eyes*. Oxford, NY, USA: Oxford University Press.

Le, S. Q. and Gascuel, O. (2008). An improved general amino acid replacement matrix. *Mol. Biol. Evol.* **25**, 1307-1320.

Liénard, M. A., Bernard, G. D., Allen, A., Lassance, J., Song, S., Childers, R., Yu, N., Ye, D., Stephenson, A., Valencia-Montoya, W. et al. (2021). The evolution of red colour vision is linked to coordinated rhodopsin tuning in lycaenid butterflies. *Proc. Natl. Acad. Sci. USA.* **118**, e2008986118.

Liénard, M. A., Valencia-Montoya, W. A. and Pierce, N. E. (2022). Molecular advances to study the function, evolution and spectral tuning of arthropod visual opsins. *Philos. Trans. R. Soc. Lond. B Biol. Sci.* **377**, 20210279.

Liu, Y., Chi, H., Li, L., Rossiter, S. J. and Zhang, S. (2018). Molecular data support an early shift to an intermediate-light niche in the evolution of mammals. *Mol. Biol. Evol.* **35**, 1130-1134.

Macias-Muñoz, A., Rangel Olguin, A. G. and Briscoe, A. D. (2019). Evolution of phototransduction genes in Lepidoptera. *Genome Biol. Evol.* **11**, 2107-2124.

Mackin, K. A., Roy, R. A., Theobald, D. L. (2014). An empirical test of convergent evolution in rhodopsins. *Mol. Biol. Evol.* **31**, 85-95.

Madej, T., Lanczycki, C. J., Zhang, D., Thiessen, P. A., Geer, R. C., Marchler-Bauer, A. and Bryant, S. H. (2014). MMDB and VAST+: tracking structural similarities between macromolecular complexes. *Nucleic Acids Res.* **42**, D297-D303.

Manni, M., Berkeley, M. R., Seppey, M., Simão, F. A. and Zdobnov, E. M. (2021). BUSCO update: novel and streamlined workflows along with broader and deeper phylogenetic coverage for scoring of eukaryotic, prokaryotic, and viral genomes. *Mol. Biol. Evol.* **38**, 4647-4654.

Maor, R., Dayan, T., Ferguson-Gow, H. and Jones, K. E. (2017). Temporal niche expansion in mammals from a nocturnal ancestor after dinosaur extinction. *Nat. Ecol. Evol.* **1**, 1889-1895.

Martin, C. H. and Richards E. J. (2019). The paradox behind the pattern of rapid adaptive radiation: how can the speciation process sustain itself through an early burst? *Annu. Rev. Ecol. Evol. Syst.* **50**, 569-593.

Matsushita, A., Awata, H., Wakakuwa, M., Takemura, S.-Y. and Arikawa, K. (2012). Rhabdom evolution in butterflies: insights from the uniquely tiered and heterogeneous ommatidia of the Glacial Apollo butterfly, *Parnassius glacialis*. *Proc. Biol. Sci.* **279**, 3482-3490.

McCulloch, K. J., Macias-Muñoz, A., Mortazavi, A. and Briscoe, A. D. (2022). Multiple mechanisms of photoreceptor spectral tuning in *Heliconius* butterflies. *Mol. Biol. Evol.* **39**, msac067.

Menzel, R. (1979). Spectral sensitivity and color vision in invertebrates. In *Comparative Physiology and Evolution of Vision in Invertebrates*. In *Handbook of Sensory Physiology* (ed. H. Autrum), vol. 7 / 6 / 6 A, pp. 503-580. Berlin and Heidelberg, Germany: Springer.

Mortazavi, A., Williams, B. A., McCue, K., Schaeffer, L. and Wold, B. (2008). Mapping and quantifying mammalian transcriptomes by RNA-Seq. *Nat. Methods* **5**, 621-628.

Naka, K. I. and Rushton, W. A. H. (1966). An attempt to analyse colour reception by electrophysiology. *J. Physiol.* **185**, 556-586.

Nei, M. and Kumar, S. (2000). *Molecular Evolution and Phylogenetics*. New York, NY, USA: Oxford University Press.

Nguyen, L.-T., Schmidt, H. A., von Haeseler, A. and Minh, B. Q. (2015). IQ-TREE: A fast and effective stochastic algorithm for estimating maximum-likelihood phylogenies. *Mol. Biol. Evol.* **32**, 268-274.

Nilsson, D.-E. (1989). Optics and evolution of the compound eye. In *Facets of Vision* (eds. D. G. Stavenga and R. C. Hardie), pp. 30-73. Berlin and Heidelberg, Germany: Springer.

R Core Team (2017). *R: A Language and Environment for Statistical Computing*. Vienna, Austria: R Foundation for Statistical Computing. https://www.R-project.org/.

Saito, T., Koyanagi, M., Sugihara, T., Nagata, T., Arikawa, K. and Terakita, A. (2019). Spectral tuning mediated by helix III in butterfly long wavelength-sensitive visual opsins revealed by heterologous action spectroscopy. *Zoological Lett.* **5**, 35.

Satoh, A., Stewart, F. J., Koshitaka, H., Akashi, H. D., Pirih, P., Sato, Y. and Arikawa, K. (2017). Red-shift of spectral sensitivity due to screening pigment migration in the eyes of a moth, *Adoxophyes orana*. *Zoological Lett.* **3**, 14.

Schwartz, R. S., Harkins, K. M., Stone, A. C. and Cartwright, R. A. (2015). A composite genome approach to identify phylogenetically informative data from next-generation sequencing. *BMC Bioinformatics* **16**, 193.

Shimodaira, H. (2002). An approximately unbiased test of phylogenetic tree selection. *Syst. Biol.* **51**, 492-508.

Sondhi, Y., Ellis, E. A., Bybee, S. M., Theobald, J. C. and Kawahara, A. Y. (2021). Light environment drives evolution of color vision genes in butterflies and moths. *Commun. Biol.* **4**, 177.

Sonnhammer, E. L. L., von Heijne, G. and Krogh, A. (1998). A hidden Markov model for predicting transmembrane helices in protein sequences. *Proc. Int. Conf. Intell. Syst. Mol. Biol.* **6**, 175-182.

Stavenga, D. G. (1995). Insect retinal pigments: Spectral characteristics and physiological functions. *Prog. Retin. Eye Res.* **15**, 231-259.

Stavenga, D. G. (2010). On visual pigment templates and the spectral shape of invertebrate rhodopsins and metarhodopsins. *J. Comp. Physiol. A* **196**, 869-878.

Stavenga, D. G. and Arikawa, K. (2011). Photoreceptor spectral sensitivities of the Small White butterfly *Pieris rapae crucivora* interpreted with optical modeling. *J. Comp. Physiol. A* **197**, 373-385.

Stavenga, D. G., Smits, R. P. and Hoenders, B. J. (1993). Simple exponential functions describing the absorbance bands of visual pigment spectra. *Vision Res.* **33**, 1011-1017.

Stewart, C.-B., Schilling, J. W. and Wilson, A. C. (1987). Adaptive evolution in the stomach lysozymes of foregut fermenters. *Nature* **330**, 401-404.

Stewart, F. J., Kinoshita, M. and Arikawa, K. (2015). The butterfly *Papilio xuthus* detects visual motion using chromatic contrast. *Biol. Lett.* **11**, 20150687.

Stöckl, A., Heinze, S., Charalabidis, A., el Jundi, B., Warrant, E. and Kelber, A. (2016). Differential investment in visual and olfactory brain areas reflects behavioural choices in hawk moths. *Sci. Rep.* **6**, 26041.

Stöckl, A., Smolka, J., O'Carroll, D. and Warrant, E. (2017). Resolving the trade-off between visual sensitivity and spatial acuity—lessons from hawkmoths. *Integr. Comp. Biol.* **57**, 1093-1103.

Sugihara, T., Nagata, T., Mason, B., Koyanagi, M. and Terakita, A. (2016). Absorption characteristics of vertebrate non-visual opsin, Opn3. *PLoS One* **11**, e0161215.

Surridge, A. K., Osorio, D. and Mundy, N. I. (2003). Evolution and selection of trichromatic vision in primates. *Trends Ecol. Evol.* **18**, 198-205.

Swanson, K. W., Irwin, D. M. and Wilson, A. C. (1991). Stomach lysozyme gene of the langur monkey: tests for convergence and positive selection. *J. Mol. Evol.* **33**, 418-425.

Telles, F. J., Kelber, A. and Rodríguez-Gironés, M. A. (2016). Wavelength discrimination in the hummingbird hawkmoth *Macroglossum stellatarum*. *J. Exp. Biol.* **219**, 553-560.

Telles, F. J., Lind, O., Henze, M. J., Rodríguez-Gironés, M. A., Goyret, J. and Kelber, A. (2014). Out of the blue: the spectral sensitivity of hummingbird hawkmoths. *J. Comp. Physiol. A* **200**, 537-546.

Terai, Y. and Okada, N. (2011). Speciation of cichlid fishes by sensory drive. In *From Genes to Animal Behavior: Social Structures, Personalities, Communication by Color* (eds. M. Inoue-Murayama, S. Kawamura and A. Weiss). In *Primatology Monographs* (eds. T. Matsuzawa and J. Yamagiwa), pp. 311-328. Tokyo, Japan: Springer.

Terakita, A. (2005). The opsins. *Genome Biol.* **6**, 213.

Thompson, J. D., Higgins, D. G. and Gibson, T. J. (1994). CLUSTAL W: improving the sensitivity of progressive multiple sequence alignment through sequence weighting, position-specific gap penalties and weight matrix choice. *Nucleic Acids Res.* **22**, 4673-4680.

van der Kooi, C. J., Stavenga, D. G., Arikawa, K., Belušič, G. and Kelber, A. (2021). Evolution of insect color vision: From spectral sensitivity to visual ecology. *Annu. Rev. Entomol.* **66**, 435-461.

Varma, N., Mutt, E., Mühle, J., Panneels, V., Terakita, A., Deupi, X., Nogly, P., Schertler, G. F. X. and Lesca, E. (2019). Crystal structure of jumping spider rhodopsin-1 as a light sensitive GPCR. *Proc. Natl. Acad. Sci. USA* **116**, 14547-14556.

von Helversen, O. (1972). Zur spektralen Unterschiedsempfindlichkeit der Honigbiene. *Journal of Comparative Physiology* **80**, 439-472. (in German).

Wakakuwa, M., Terakita, A., Koyanagi, M., Stavenga, D. G., Shichida, Y. and Arikawa, K. (2010). Evolution and mechanism of spectral tuning of blue-absorbing visual pigments in butterflies. *PLoS One* **5**, e15015.

Wakakuwa, M., Stewart, F., Matsumoto, Y., Matsunaga, S. and Arikawa, K. (2014). Physiological basis of phototaxis to near-infrared light in *Nephotettix cincticeps*. *J. Comp. Physiol. A* **200**, 527-536.

Walls, G. L. (1942). *The Vertebrate Eye and Its Adaptive Radiation*. Bloomfield Hills, MI, USA: Cranbrook Institute of Science.

Wang, J., Youkharibache, P., Zhang, D., Lanczycki, C. J., Geer, R. C., Madej, T., Phan, L., Ward, M., Lu, S., Marchler, G. H. et al. (2020). iCn3D, a web-based 3D viewer for sharing 1D/2D/3D representations of biomolecular structures. *Bioinformatics* **36**, 131-135.

Warrant, E., Bartsch, K. and Günther, C. (1999). Physiological optics in the hummingbird hawkmoth: a compound eye without ommatidia. *J. Exp. Biol.* **202**, 497-511.

White, R. H., Xu, H., Münch, T. A., Bennett, R. R. and Grable, E. A. (2003). The retina of *Manduca sexta*: rhodopsin expression, the mosaic of green-, blue- and UV-sensitive photoreceptors, and regional specialization. *J. Exp. Biol.* **206**, 3337-3348.

Xu, B. and Yang, Z. (2013). PAMLX: a graphical user interface for PAML. *Mol. Biol. Evol.* **30**, 2723-2724.

Xu, P., Lu, B., Xiao, H., Fu, X., Murphy, R. W. and Wu, K. (2013). The evolution and expression of the moth visual opsin family. *PLoS One* **8**, e78140.

Yamaguchi, S., Wolf, R., Desplan, C. and Heisenberg, M. (2008). Motion vision is independent of color in *Drosophila*. *Proc. Natl. Acad. Sci. USA* **105**, 4910-4915.

Yan, S., Zhu, J., Zhu, W., Zhang, X., Li, Z., Liu, X. and Zhang, Q. (2014). The expression of three opsin genes from the compound eye of *Helicoverpa armigera* (Lepidoptera: Noctuidae) is regulated by a circadian clock, light conditions and nutritional status. *PLoS One.* **9**, e111683.

Yang, Z. (1997). PAML: a program package for phylogenetic analysis by maximum likelihood. *Comput. Appl. Biosci.* **13**, 555-556.

Yang, Z. (2007). PAML 4: phylogenetic analysis by maximum likelihood. *Mol. Biol. Evol.* **24**, 1586-1591.

Yau, K.-W. and Hardie, R. C. (2009). Phototransduction motifs and variations. *Cell.* 139, 246-264.

Yokoyama, S. (2000). Molecular evolution of vertebrate visual pigments. *Prog. Retin. Eye Res.* **19**, 385-419.

Yokoyama, S. (2008). Evolution of dim-light and color vision pigments. *Annu. Rev. Genomics Hum. Genet.* **9**, 259-282.

Zhang, J. and Kumar, S. (1997). Detection of convergent and parallel evolution at the amino acid sequence level. *Mol. Biol. Evol.* **14**, 527-536.

Zhang, J. and Nei, M. (1997). Accuracies of ancestral amino acid sequences inferred by the parsimony, likelihood, and distance methods. *J. Mol. Evol.* **44**, S139-S146.

Zuckerkandl, E. and Pauling, L. (1965). Evolutionary divergence and convergence in proteins, In *Evolving Genes and Proteins* (eds. V. Bryson and H. Vogel), pp. 97-166. New York, NY, USA: Academic Press.